Development 138, 431-441 (2011) doi:10.1242/dev.053843

Lineage tracing reveals the dynamic contribution of *Hes1*$^{+}$ cells to the developing and adult pancreas

Daniel Kopinke[1], Marisa Brailsford[1], Jill E. Shea[2], Rebecca Leavitt[1], Courtney L. Scaife[2] and L. Charles Murtaugh[1,*]

SUMMARY

Notch signaling regulates numerous developmental processes, often acting either to promote one cell fate over another or else to inhibit differentiation altogether. In the embryonic pancreas, Notch and its target gene *Hes1* are thought to inhibit endocrine and exocrine specification. Although differentiated cells appear to downregulate *Hes1*, it is unknown whether *Hes1* expression marks multipotent progenitors, or else lineage-restricted precursors. Moreover, although rare cells of the adult pancreas express *Hes1*, it is unknown whether these represent a specialized progenitor-like population. To address these issues, we developed a mouse *Hes1*^{CreERT2} knock-in allele to inducibly mark *Hes1*$^{+}$ cells and their descendants. We find that *Hes1* expression in the early embryonic pancreas identifies multipotent, Notch-responsive progenitors, differentiation of which is blocked by activated Notch. In later embryogenesis, *Hes1* marks exocrine-restricted progenitors, in which activated Notch promotes ductal differentiation. In the adult pancreas, *Hes1* expression persists in rare differentiated cells, particularly terminal duct or centroacinar cells. Although we find that *Hes1*$^{+}$ cells in the resting or injured pancreas do not behave as adult stem cells for insulin-producing beta (β)-cells, *Hes1* expression does identify stem cells throughout the small and large intestine. Together, these studies clarify the roles of Notch and *Hes1* in the developing and adult pancreas, and open new avenues to study Notch signaling in this and other tissues.

KEY WORDS: Pancreas, Hes1, Notch, Stem cell, Mouse

INTRODUCTION

The vertebrate pancreas comprises three major cell types: endocrine islets, which include insulin-producing β-cells; and a network of exocrine acinar and duct cells, which are responsible for producing and transporting digestive enzymes, respectively. The Notch signaling pathway has been implicated in several aspects of pancreatic cell fate determination, beginning with the finding that mouse embryos lacking various Notch components, including the downstream target gene *Hes1*, exhibit overproduction of endocrine cells (Apelqvist et al., 1999; Jensen et al., 2000). Hes1 can repress the promoter of *Neurog3*, a crucial pro-endocrine transcription factor, and de-repression of *Neurog3* in the absence of *Hes1* may drive excessive endocrine differentiation (Apelqvist et al., 1999; Jensen et al., 2000; Lee et al., 2001). In gain-of-function experiments, Notch also inhibits exocrine acinar cell development, promoting instead progenitor maintenance (Esni et al., 2004; Hald et al., 2003; Murtaugh et al., 2003). These findings are corroborated by studies in zebrafish (Esni et al., 2004; Yee et al., 2005; Zecchin et al., 2006), and conform to a generic conception of Notch as regulating cell fate throughout animal development (Lai, 2004).

The Notch pathway knockout phenotypes implied that the early pancreas comprised multipotent cells, the differentiation of which was held in check by Notch signaling (Apelqvist et al., 1999; Jensen et al., 2000). Lineage-tracing studies suggest that multipotent progenitors reside in the 'tips' of the embryonic pancreatic epithelium, the expansion of which leaves behind 'trunks' that give rise to ducts and islets (Kopinke and Murtaugh, 2010; Solar et al., 2009; Zhou et al., 2007). How Notch regulates this process is unknown, although it may signal through *Hes1* to repress *Neurog3* (Lee et al., 2001) and control the balance of duct and islet differentiation. Contradicting this model, however, deletion of *Notch1* and *Notch2*, the major receptors expressed in the pancreas, has little effect on late embryonic islet development (Nakhai et al., 2008).

Whether progenitor cells persist in the adult pancreas, particularly for insulin-producing β-cells, remains controversial. Two lineage tracing approaches have been taken to address this issue: 'pulse-chase' labeling of mature islet cells, to detect changes in labeling frequency caused by differentiation of new β-cells (neogenesis); or marking acini and/or ducts, to determine whether they can contribute to β-cells. The former studies argue against β-cell neogenesis (Dor et al., 2004), and the latter indicate that neogenesis is either non-existent (Desai et al., 2007; Kopinke and Murtaugh, 2010; Solar et al., 2009) or rare (Inada et al., 2008) in the uninjured pancreas. Pancreatic injury, in particular caused by ligation of the main duct, has been proposed to induce facultative neogenesis from acinar or duct cells (Wang et al., 1995; Xu et al., 2008), for which exist both contradictory and supporting lineage tracing data (Inada et al., 2008; Solar et al., 2009). As previous approaches used mature duct or acinar marker genes to drive Cre expression, however, they may have excluded specialized adult progenitor cells. These might include centroacinar cells, terminal elements of the exocrine ductal network in which Notch-*Hes1* signaling appears particularly high

[1]Department of Human Genetics, University of Utah School of Medicine, Salt Lake City, UT 84112, USA. [2]Department of Surgery, University of Utah School of Medicine, Salt Lake City, UT 84132, USA.

*Author for correspondence (murtaugh@genetics.utah.edu)

Accepted 22 November 2010

(Miyamoto et al., 2003; Parsons et al., 2009; Stanger et al., 2005). These cells have been suggested to generate new β-cells following injury (Hayashi et al., 2003; Nagasao et al., 2003), and they can give rise to both acinar and islet cells following isolation and culture (Rovira et al., 2010).

To understand how and when Notch-*Hes1* signaling regulates pancreatic progenitor cells, we generated 'knock-in' mice in which the tamoxifen-dependent CreERT2 recombinase is targeted to the *Hes1* locus. With these mice, we have analyzed the stage-specific differentiation potential of Notch-responsive cells in the embryonic pancreas, revealing a novel shift from multipotent to exocrine-restricted progenitor cells. This parallels a shift in the cellular response to Notch, from arresting differentiation to promoting duct cell specification. In the adult, we find that *Hes1*$^{+}$ duct and centroacinar cells appear to be fixed in their fate, and do not detectably contribute to β-cells, even after duct ligation injury. Ours is the first study to address the fate of Notch-responsive cells in any adult tissue, and supports an emerging model that lineage boundaries in the pancreas are normally fixed at birth.

MATERIALS AND METHODS

Mice

We used bacterial recombineering (Liu et al., 2003) to generate a *Hes1*$^{CreERT2\text{-}neoR}$ targeting vector, in which most of the *Hes1* open reading frame, including the bHLH domain, is replaced by that of *CreERT2* (Feil et al., 1997), linked to an FRT-flanked *neo*^{R} cassette (see Fig. S1A in the supplementary material). This was electroporated into R1 ES cells (Nagy et al., 1993), generously provided by Mario Capecchi (University of Utah, USA), and G418-resistant ES cell clones were screened by Southern blotting and PCR (see Fig. S1B in the supplementary material and data not shown). Germline chimeras were derived by the University of Utah Transgenic Core Facility. The *neo*^{R} cassette was excised in vivo by breeding to *Rosa26*^{FLPe} (Farley et al., 2000), obtained from the Jackson Laboratory. Cre reporter mice *R26R*^{EYFP} (Srinivas et al., 2001) and *R26R*^{LacZ} (Soriano, 1999) were obtained from the Jackson Laboratory. *Rosa26*^{NIC} (Murtaugh et al., 2003) and *Pdx1Cre* mice (Gu et al., 2002) were provided by Doug Melton (Harvard University, MA, USA). *Ctnnb1*$^{lox(ex3)}$ mice (Harada et al., 1999) were provided by Makoto Mark Taketo (Kyoto University, Japan). Tamoxifen (Sigma T-5648) was dissolved in corn oil and administered by oral gavage.

Explant cultures were established from E11.5 dorsal pancreatic buds, with embryos genotyped by PCR immediately after dissection. Buds were cultured at the air-medium interface, on Millicell-CM filters (0.4 μm pore size; Millipore), in DMEM supplemented with 10% FBS and antibiotics. As indicated, explants were treated with the γ-secretase inhibitor DAPT (10 μM final; Calbiochem) to inhibit Notch signaling (Dovey et al., 2001), or with vehicle alone as a control (0.1% DMSO final), 24 hours prior to treatment with 250 nM 4-hydroxytamoxifen to activate CreERT2.

Pancreatic duct ligations were performed as described previously (Scoggins et al., 2000; Solar et al., 2009; Xu et al., 2008), following a protocol approved by the University of Utah IACUC. Briefly, following midline laparotomy, the stomach and ascending colon were deflected to access the dorsal pancreas. The dorsal pancreas was lifted and stretched slightly with a surgical probe, and a monofilament ligature placed near the base, sparing the splenic vessels. Surgery was performed under isoflurane anesthesia, and mice received an analgesic dose of buprenorphine (50 μg/kg body weight) immediately after surgery.

Immunostaining and lineage analysis

Tissues were fixed and immunostained essentially as described previously (Kopinke and Murtaugh, 2010). Immunofluorescence was performed on frozen sections (7-8 μm) of tissue fixed in 4% paraformaldehyde/PBS (4°C, 1-2 hours). Other analyses used paraffin sections (6 μm) of tissue fixed in zinc-buffered formalin (room temperature, overnight). Primary antibodies used in this study are listed in Table 1; where indicated, sections were also stained with Dolichos biflorus agglutinin (DBA) lectin (Vector Laboratories), which marks duct cells (Kobayashi et al., 2002). Staining was analyzed by compound fluorescent or light microscopy, using MicroSuite software (Olympus). Photomicrographic images were processed using Adobe Photoshop, with parallel images processed identically.

Our lineage analysis approach, following that of others (Gu et al., 2002; Solar et al., 2009; Zhou et al., 2007), is schematized in Fig. S2 in the supplementary material. One or two randomly chosen fields, comprising 800-1000 DAPI^{+} cells each, were photographed from each of four to ten widely separated sections. For studies of E17.5 embryonic pancreata, we collected six to eight sections per slide, separated by 80-100 μm and spanning the entire pancreas as well as adjacent stomach and duodenum. For uninjured adult pancreata, we embedded and sectioned one half of each dorsal pancreas, collecting four or five sections per slide spaced at least 100 μm apart. For duct ligations, we sectioned the entire dorsal pancreas (ligated and unligated regions), collecting eight to ten sections per slide separated by at least 120 μm. Total numbers of mice, fields and cells scored in each experiment are listed in Tables S2 and S3 in the supplementary material.

Labeling efficiencies were derived from co-immunofluorescence, using the Analyze Particles function of ImageJ (NIH) (Kopinke and Murtaugh, 2010). Counting accuracy was confirmed by eye in Adobe Photoshop for random samples. To exclude the possibility that cells were scored incorrectly due to poor resolving power of the compound microscope, two samples were scored according to the same criteria but using optical sections (less than 1 μm thick) generated by confocal microscopy (Fig. 3). Calculations and graphs were generated with Microsoft Excel and R (www.r-project.org).

Table 1. Primary antibodies used in this study

Antigen	Species	Source	Catalog number	Dilution
Amylase	Sheep	BioGenesis	0480-0104	1:2500
Amylase	Rabbit	Sigma	A8273	1:1000
Cytokeratin-19	Rat	Developmental Studies Hybridoma Bank	TROMA-3	1:50
Cpa1	Goat	R&D systems	AF2765	1:2000
C-peptide (insulin)	Rabbit	Linco	4020-01	1:2500
C-peptide (insulin)	Goat	Linco	4023-01	1:5000
Cre	Mouse	Millipore	MAB3120	1:500
E-cadherin	Rat	Zymed/Invitrogen	13-1900	1:2000
GFP	Rabbit	Abcam	ab290	1:4000
GFP	Goat	Rockland	600-101-215	1:2500
Glucagon	Rabbit	Zymed / Invitrogen	18-0064	1:250
Glucagon	Guinea pig	Linco	4031-01F	1:2500
Hes1	Rabbit	Nadean Brown (University of Cincinnati, OH, USA)		1:1000
Ki67	Rabbit	Vector labs	VP-RM04	1:150
Pdx1	Guinea pig	Chris Wright (Vanderbilt University, TN, USA)		1:10,000
PECAM	Rat	BD Pharmingen	553370	1:125
Somatostatin	Goat	Santa Cruz	sc-7819	1:500

RESULTS

Hes1 expression and gene targeting

To extend previous studies of *Hes1* expression (Apelqvist et al., 1999; Esni et al., 2004; Jensen et al., 2000; Lammert et al., 2000), we performed Hes1 immunostaining on pancreata of different embryonic stages, spanning major developmental transitions. At E11.5, when most cells are undifferentiated progenitors, we found widespread but non-uniform expression of Hes1 in the epithelium (Fig. 1A), consistent with previous immunostaining and in situ hybridization studies (Jensen et al., 2000; Lammert et al., 2000; Murtaugh et al., 2005; Nakhai et al., 2008). We observed Hes1 downregulation from E13.5, the onset of the 'secondary transition' wave of acinar and β-cell differentiation (Gittes, 2009; Pictet and Rutter, 1972). Hes1 was initially mosaic throughout the epithelium (Fig. 1B), partly overlapping with the 'tip cell' marker carboxypeptidase A1 (Cpa1) (see Fig. S3A in the supplementary material) (Zhou et al., 2007), but became increasingly confined to Cpa1-negative ductal and centroacinar cells at later stages (Fig. 1C-D; Fig. S3B,C in the supplementary material). A similar restriction of Hes1 from tip cells has been seen previously (Esni et al., 2004), and the late ductal localization prefigures its expression in the adult (Miyamoto et al., 2003; Stanger et al., 2005). Antibody specificity was indicated by the lack of staining in *Hes1*-deficient embryos (generated as described below) (see Fig. S3D,E in the supplementary material). Together, these data unify previous studies, and support the hypothesis that Hes1 expression marks early pancreatic progenitors (Esni et al., 2004; Jensen et al., 2000).

In order to follow the fate of *Hes1*$^{+}$ cells, we engineered a *Hes1*^{CreERT2} allele (henceforth, *Hes1*^{C2}) by replacing most of the coding region with *CreERT2*, a tamoxifen-inducible recombinase (Feil et al., 1997) (Fig. 1E; Fig. S1 in the supplementary material). *Hes1*$^{C2/+}$ animals were viable and fertile, while most *Hes1*$^{C2/C2}$ embryos died between E12.5 and E13.5 (data not shown), as described for *Hes1* knockouts (Ishibashi et al., 1995).

To confirm that *Hes1*^{C2} was active in *Hes1*-expressing cells, we immunostained for Hes1, Cre and *lacZ* in E12.5 embryos double-transgenic for *Hes1*^{C2} and the lineage reporter *R26R*^{LacZ} (Soriano, 1999), which had received tamoxifen (TM) by maternal gavage at E9.5. We observed close overlap between Cre and Hes1 (see Fig. S4A-F in the supplementary material), indicating that *Hes1*^{C2} recapitulates endogenous *Hes1* expression. Furthermore, the *lacZ* lineage marker was widely expressed in the pancreatic epithelium, including by numerous cells that continue to express Hes1 (see Fig. S4G-I, arrowheads, in the supplementary material). In organ cultures, 4-hydroxytamoxifen treatment of dorsal pancreatic buds from E11.5 embryos double-transgenic for *Hes1*^{C2} and the lineage reporter *R26R*^{EYFP} (Srinivas et al., 2001) induced widespread epithelial EYFP expression. Labeling was almost abolished by pre-treatment with the γ-secretase inhibitor DAPT (Dovey et al., 2001) (see Fig. S5 in the supplementary material), indicating that *Hes1*^{C2} expression requires Notch activity. Together, these results indicate that *Hes1*^{C2} is expressed and regulated in the same way as endogenous *Hes1*, and that *Hes1*^{C2} can be used to follow the fate of Notch-responsive cells.

Progressive lineage restriction of embryonic *Hes1*$^{+}$ pancreatic progenitor cells

We performed additional crosses between *Hes1*^{C2} and *R26R*^{LacZ}, administered a single 2 mg tamoxifen dose to pregnant females between E9.5 and E15.5, and analyzed *lacZ* expression in the pancreas and gut at E17.5 (n=3-5 embryos per treatment group). No recombination was detected in the absence of tamoxifen (Fig. 2A,F). The labeling frequency in the pancreas was highest (~25%) when tamoxifen was given at E9.5 (Fig. 2B), and decreased with later treatment: ~12% *lacZ*$^{+}$ with TM at E11.5, ~8% at E13.5 and ~5% at E15.5 (Fig. 2C-E). [In this and other experiments, we analyzed multiple sections spaced throughout the specimen, to avoid errors due to stochastic variations in labeling efficiency (see Fig. S2 in the supplementary material).] The *Hes1*^{C2} labeling pattern agrees with the downregulation of endogenous Hes1 expression (Fig. 1A-D), and was reproduced using the *R26R*^{EYFP} reporter (data not shown). In contrast to the pancreas, liver labeling by *Hes1*^{C2} increased with later tamoxifen administration, particularly in cells adjacent to the portal veins (Fig. 2F-J). Almost all labeled cells in the liver expressed the ductal plate markers CK19 and E-cadherin (see Fig. S6 in the supplementary material and data not shown), consistent with studies showing that Notch and Hes1 promote intrahepatic bile duct development (Antoniou et al., 2009; Geisler et al., 2008; Kodama et al., 2004; Lozier et al., 2008; Zong et al., 2009).

To determine the fate of *Hes1*^{C2}-labeled cells in the pancreas, we stained these specimens for endocrine and exocrine differentiation markers, and calculated the fraction of labeled (*lacZ*$^{+}$) cells expressing each marker. Scoring over 1000 *lacZ*$^{+}$ cells in each experimental group (see Table S1 in the supplementary material), we found that *Hes1*$^{+}$ cells labeled at E9.5 generate both endocrine and exocrine progeny, with roughly one-third of all *lacZ*$^{+}$ cells co-expressing insulin (β-cells) or glucagon (α-cells), and the remainder comprising amylase^{+} acinar and DBA^{+} duct cells (Fig. 3A-D,I-J). [Note that although these counts were derived from images taken on a compound microscope, we obtained essentially identical numbers with images generated by confocal microscopy

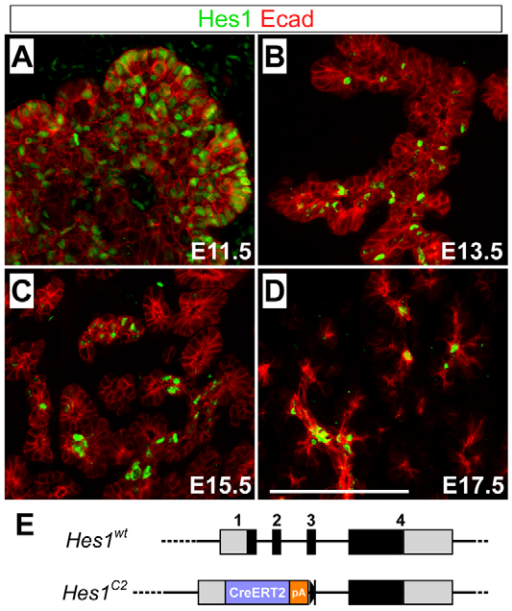

Fig. 1. Hes1 expression and targeting. (**A-D**) Staining for Hes1 (green) and the epithelial marker E-cadherin (red), in embryonic pancreata of the indicated stages. Scale bar: 100 μm. (**E**) Schematic of wild-type and targeted *Hes1*. The wild-type *Hes1* locus is depicted at the top (exons boxed and numbered, UTRs in grey and coding regions in black), for comparison with *Hes1*^{C2}, in which the *CreERT2* gene and bovine growth hormone polyadenylation signal (pA) are placed in-frame with the *Hes1* start codon, replacing much of the ORF.

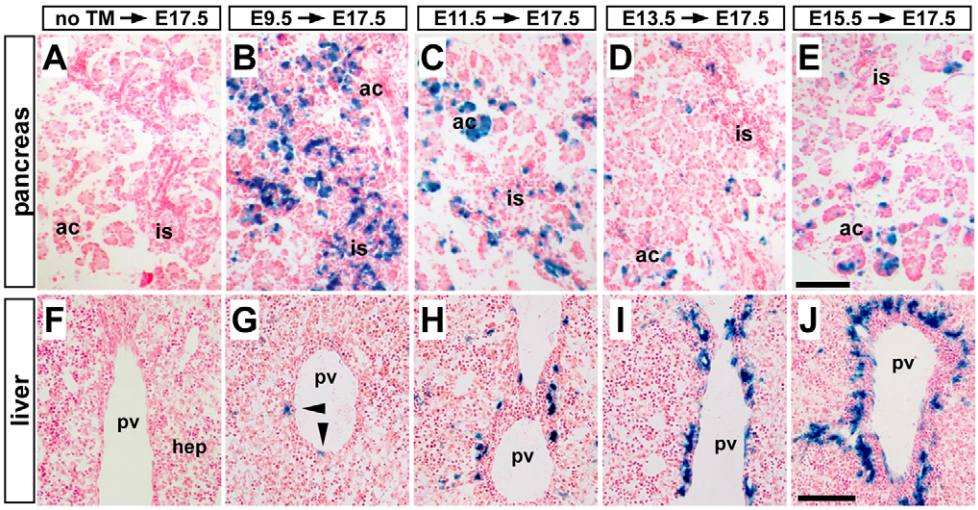

Fig. 2. Dynamic contribution of *Hes1*$^{+}$ cells to developing pancreas and liver. X-gal-stained sections of pancreas (**A-E**) or liver (**F-J**) from E17.5 *Hes1*$^{C2/+}$; *R26R*$^{LacZ/+}$ embryos that received no tamoxifen, or that received a single TM dose between E9.5 and E15.5. *lacZ*$^{+}$ cells stain blue, and sections are counterstained with Nuclear Fast Red. No recombination occurs without TM (A,F), whereas TM at E9.5 labels many pancreatic acinar (ac) and islet (is) cells (B). Pancreatic labeling declines with later TM treatment (C-E), whereas the opposite pattern is observed in the liver, where *lacZ*$^{+}$ cells are found near the portal veins (pv, arrowhead) (G-J). Few hepatocytes (hep) are labeled at any stage. Scale bars: 100 μm.

(Fig. 3I-J).] This finding implies that early *Hes1*$^{+}$ cells are multipotent, a conclusion supported by a low-dose clonal labeling approach, previously used to demonstrate tip cell multipotency (Zhou et al., 2007) (see Fig. S7 in the supplementary material). Together, these results are consistent with Notch signaling through *Hes1* to maintain early multipotent progenitors.

Later *Hes1*$^{+}$ cells continued to generate exocrine progeny, while appearing to lose endocrine differentiation capacity: almost no α-cells were labeled by TM treatment at E13.5, and β-cell labeling approached zero at E15.5 (Fig. 3E-J). Reduced islet contribution was also seen when comparing E13.5-labeled pancreata, 2 weeks after birth, with those labeled at E9.5 (Fig. 3K-N). Delivery of live pups in these experiments required lower tamoxifen doses, which resulted in decreased labeling overall but did not affect the distribution of labeled cells among differentiated lineages. The fact that labeling efficiency was uncoupled from label distribution implies that *Hes1*^{C2} drives recombination within a cell population of relatively homogeneous potential for endocrine, duct and acinar differentiation, with the proportion of labeled cells depending on TM dose. We cannot exclude the existence of cells expressing *Hes1* at levels too low for labeling by *Hes1*^{C2}, the developmental potential of which might differ from those observed here. Nonetheless, our results suggest that *Hes1* expression shifts from multipotent to exocrine-restricted progenitors (Fig. 3O), consistent with *Hes1* having to turn off before the pro-endocrine gene *Neurog3* can turn on (Jensen et al., 2000; Lee et al., 2001).

Ectopic Notch activation blocks differentiation of early but not late *Hes1*$^{+}$ cells

The wave of acinar and islet cell differentiation that occurs at the secondary transition coincides with *Hes1* downregulation (Fig. 1A-D), and we have previously shown that artificially preventing Notch downregulation blocks this differentiation process (Murtaugh et al., 2003). This was achieved by crossing the pan-pancreatic driver *Pdx1Cre* (Gu et al., 2002) to *Rosa26*$^{Notch1IC\text{-}IRES\text{-}GFP}$ (henceforth, *Rosa26*^{NIC}), which drives co-expression of activated mouse Notch1 and GFP (Murtaugh et al., 2003) (Fig. 4A,G). To determine whether early and late *Hes1*$^{+}$ cells are similarly susceptible to Notch, we crossed *Hes1*^{C2} to *Rosa26*^{NIC}.

Pregnant females received a single 2 mg TM dose between E9.5 and E15.5, and double-transgenic offspring were analyzed at E17.5 (n=2 or 3 per timepoint, see Table S1 in the supplementary material). After TM at E9.5 or E11.5, GFP^{+} cells (expressing activated Notch) formed cystic structures lacking endocrine or acinar marker expression (Fig. 4B-C,H-I). This phenotype resembled that obtained with *Pdx1Cre* (Fig. 4A,G), and agrees with early *Hes1*$^{+}$ cells representing multipotent, Notch-sensitive progenitors. The GFP^{+} epithelia stained with DBA lectin, which marks mature ducts as well as embryonic progenitors (Kobayashi et al., 2002), but their cystic morphology distinguished them from the narrow and highly-branched ducts normally present at these stages (Fig. 4G-K).

Although *Hes1*^{C2} labeled very few islet cells at E13.5 or E15.5 (Fig. 3I), *Rosa26*^{NIC} prevented even this low level of islet differentiation (Fig. 4D,E). By contrast, exocrine differentiation of E13.5-E15.5 *Hes1*$^{+}$ cells appeared to be partially Notch resistant, as GFP^{+} cells were found integrated into normal acini and ducts (Fig. 4J-K). To determine if the blunted effects of late *Rosa26*^{NIC} activation were secondary to the overall decrease in *Hes1*^{C2} labeling efficiency (Fig. 2), we repeated E9.5 treatment with a lower tamoxifen dose (0.5 mg), to activate fewer cells. As previously, the rare GFP^{+} cells observed in this experiment formed abnormal cystic tubules (Fig. 4F,L), suggesting that early Notch activation can disrupt exocrine differentiation without a 'critical mass' of affected cells.

When *Rosa26*^{NIC} is activated by *Pdx1Cre*, all cells exhibit a Pdx1^{high} 'trapped progenitor' phenotype (Murtaugh et al., 2003) (see Fig. S8A,D in the supplementary material). When Notch was activated by *Hes1*^{C2} at E15.5, GFP^{+} cells were negative for Pdx1, which instead was expressed only by β-cells (see Fig. S8C,F in the supplementary material). Cells in which *Rosa26*^{NIC} was induced at E9.5 exhibited modest Pdx1 upregulation (see Fig. S8B,E in the supplementary material), suggesting that they retained a partial progenitor-like identity (Fig. 4N).

Further analysis of late-induced *Hes1*$^{C2/+}$; *Rosa26*$^{NIC/+}$ pancreata revealed that Notch activation at E13.5 caused most GFP^{+} cells to adopt a ductal rather than acinar fate, whereas after E15.5 activation the proportions were reversed (Fig. 4M). The latter resembles the wild-type distribution observed with *R26R*^{LacZ} (Fig. 3J), suggesting that Notch activation at E15.5

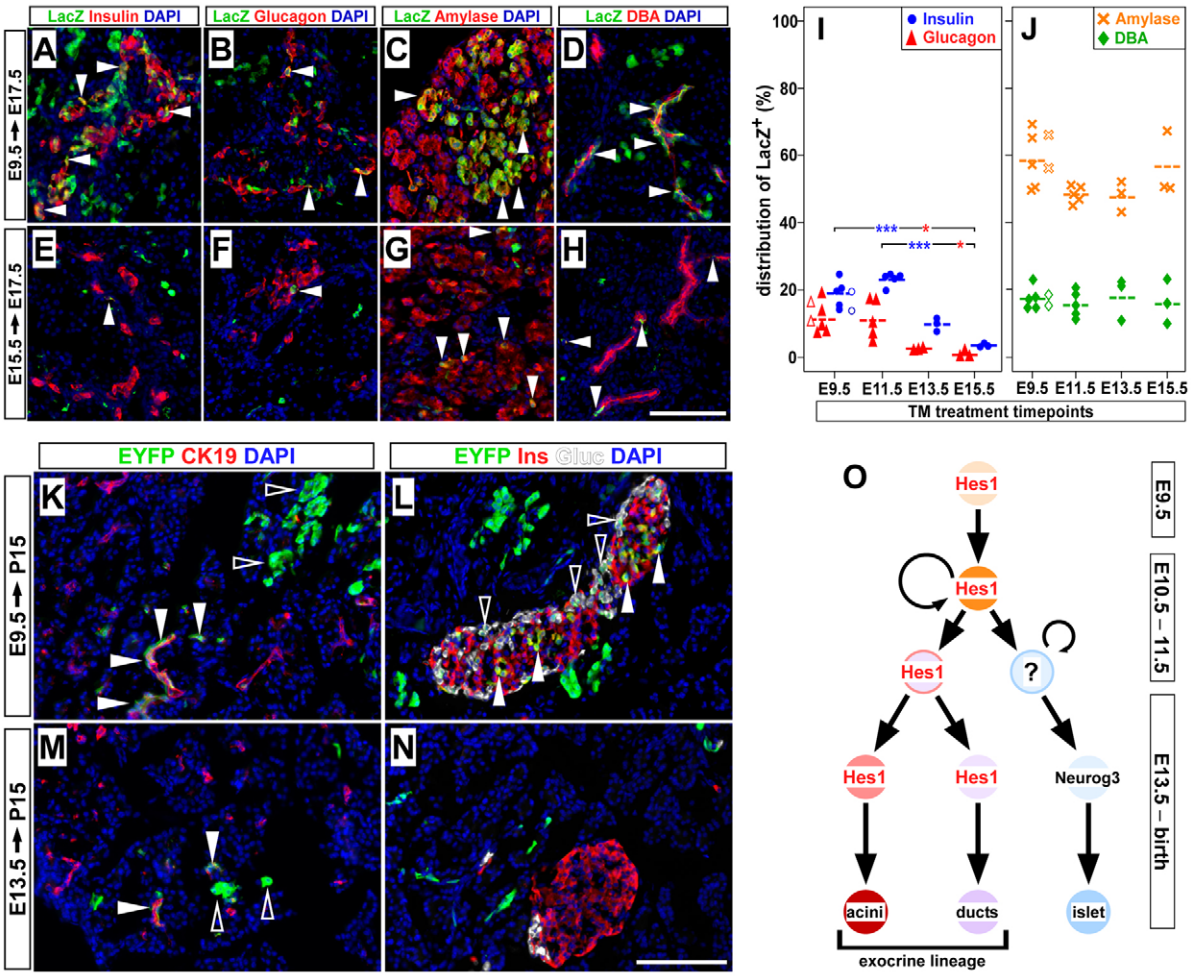

Fig. 3. Shift in differentiation potential of *Hes1*$^{+}$ cells during pancreas development. (**A-H**) *Hes1*$^{C2/+}$; *R26R*$^{LacZ/+}$ pancreata were TM labeled between E9.5 and E15.5, and analyzed at E17.5 (see Fig. 2). Staining for *lacZ* (green) and endocrine (insulin or glucagon) or exocrine (amylase or DBA) markers (red); nuclei stained with DAPI (blue). White arrowheads indicate *Hes1*^{C2}-labeled cells, which are most abundant following E9.5 labeling. Scale bar: 100 μm. (**I**,**J**) Quantitative distribution of *lacZ*$^{+}$ cells at E17.5, after TM treatment at indicated stages. Each point represents a single pancreas, in which at least five fields (300-1500 *lacZ*$^{+}$ cells) were scored for the fraction of *lacZ*$^{+}$ cells expressing the indicated marker: insulin (blue circle), glucagon (red triangle), amylase (orange X) or DBA (green diamond). Means are indicated by broken lines. Open points indicate data obtained using confocal microscopy. **P*<0.05 and ****P*<0.0005, by Tukey's HSD test. (**K-N**) *Hes1*$^{C2/+}$; *R26R*$^{EYFP/+}$ mice received TM in utero at E9.5 or E13.5 and were analyzed at P15 for co-expression of EYFP (green) with CK19 (left, red), insulin (right, red) or glucagon (right, white). *Hes1*$^{+}$ cells labeled at either stage contribute to ducts and acini (K,M, closed and open arrowheads), whereas only early *Hes1*$^{+}$ cells make significant contribution to adult β- and α-cells (L, closed and open arrowheads). Scale bar: 100 μm. (**O**) Early *Hes1*$^{+}$ cells appear to be multipotent, but become restricted to the exocrine lineage after E13.5, concomitant with the secondary transition.

does not perturb exocrine differentiation, while E13.5 activation drives bipotent progenitors toward a duct fate (Fig. 4N). Activated Notch can also respecify endocrine precursors to ducts (Greenwood et al., 2007), and this pro-ductal activity may underlie the pathological effects of Notch in pancreatic cancer (De La O et al., 2008).

Lineage tracing *Hes1*$^{+}$ cells in the adult pancreas and intestine

The question of whether pancreatic progenitor cells persist after birth is a matter of long-standing controversy, particularly with respect to adult differentiation of β-cells. Although several lineage-tracing studies indicate that adult duct and acinar cells do not generate new β-cells in the resting or regenerating pancreas (Desai et al., 2007; Kopinke and Murtaugh, 2010; Solar et al., 2009), these have not excluded the existence of specialized progenitor cells. Centroacinar cells (CACs), in particular, have been proposed to behave as β-cell progenitors (Hayashi et al., 2003; Nagasao et al., 2003; Rovira et al., 2010). CACs express higher levels of *Hes1* than do other exocrine cells (Miyamoto et al., 2003; Stanger et al., 2005), and we used *Hes1*^{C2} to determine whether these or other *Hes1*$^{+}$ cells behave as adult stem or progenitor-like cells.

To identify *Hes1*-expressing cells in the adult pancreas, we administered 10 mg tamoxifen to 2-month-old (P60) *Hes1*$^{C2/+}$; *R26R*$^{EYFP/+}$ mice (n=4), and analyzed EYFP expression ~48 hours later. Consistent with prior studies of Hes1 expression, we found EYFP labeling of approx. one-quarter of CK19^{+} centroacinar cells (Fig. 5A), as well as a lesser proportion of labeled cells within larger ducts (Fig. 5B). We also observed a small fraction of EYFP^{+} acinar cells, suggesting *Hes1* expression by rare, differentiated acinar cells (Fig. 5C). To follow the longer-term fate of adult (P60) *Hes1*$^{+}$ cells, we compared quantitatively the labeling obtained at 7 days post-TM,

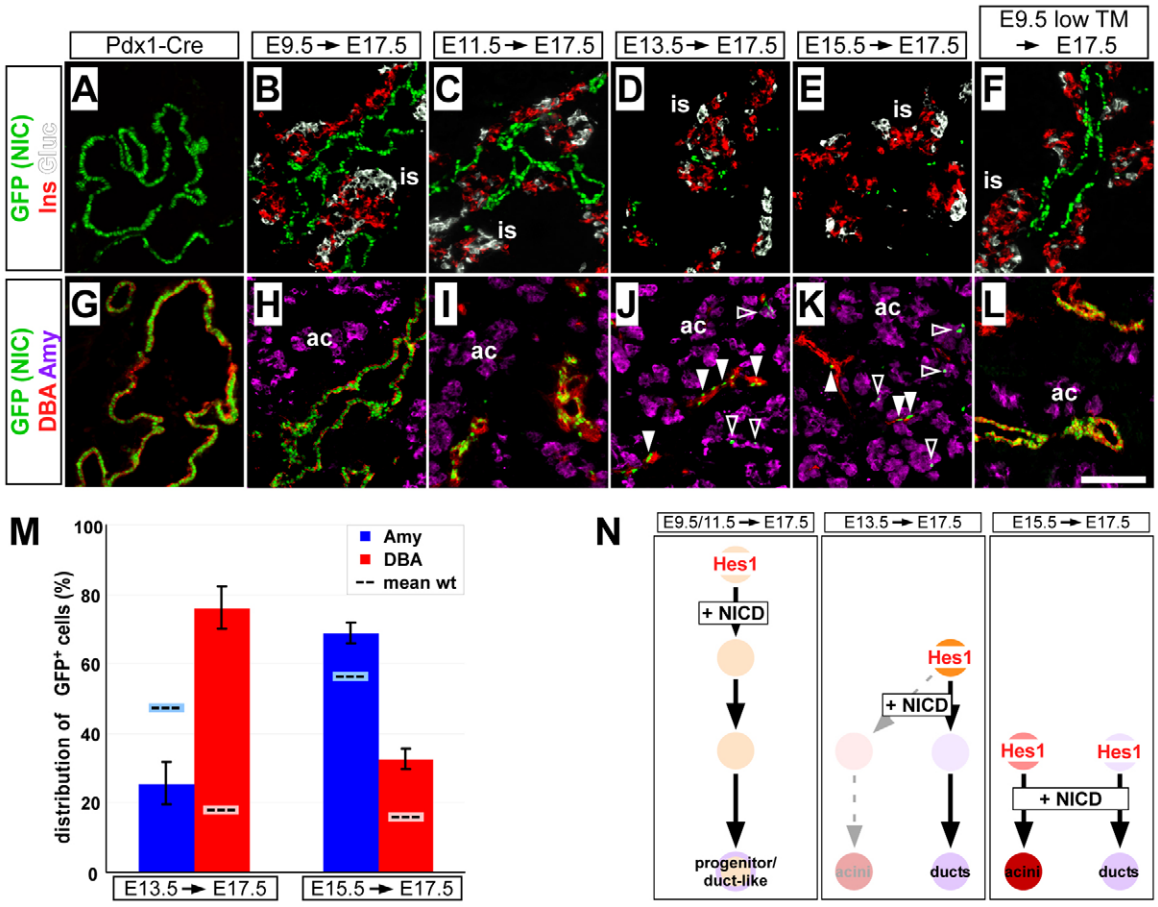

Fig. 4. Ectopic Notch activation blocks differentiation of early but not late *Hes1*$^+$ cells. (**A-L**) *Rosa26*^{NIC} was activated by *Pdx1Cre* or by *Hes1*$^{C2/+}$ following TM treatment between E9.5 and E15.5. E17.5 pancreata were stained for co-expression of GFP (green), marking *Rosa26*^{NIC} expression, with the endocrine markers insulin and glucagon (top, red and white) or exocrine markers DBA and amylase (bottom, red and purple). *Rosa26*^{NIC} activation in *Pdx1*$^+$ or E9.5 *Hes1*$^+$ cells blocks islet and acinar differentiation, and induces DBA$^+$ cysts (A,B,G,H). Lower-dose activation of *Hes1*^{C2} at E9.5 induces similar GFP$^+$ cysts (F,L). With later stage activation, GFP$^+$ cells assume an increasingly normal appearance (C-E,I-K), including integration into normal ducts and co-expression of amylase (closed and open arrowheads). Scale bar: 100 μm. (**M**) Quantitative distribution of GFP$^+$ cells among amylase$^+$ (blue) and DBA$^+$ (red) cells at E17.5, after *Rosa26*^{NIC} activation at E13.5 or E15.5 (~100 GFP$^+$ cells scored per sample). Broken lines indicate the normal distribution of *Hes1*^{C2}-labeled cells after TM treatment at these stages (from Fig. 3J). Notch activation at E13.5 promotes duct development, whereas activation at E15.5 does not perturb normal exocrine differentiation of *Hes1*$^+$ cells. Results are mean±s.e.m. (**N**) Notch activation in early (E9.5-E11.5) *Hes1*$^+$ progenitor cells (light orange) prevents normal differentiation and induces a progenitor/duct-like phenotype. At E13.5, Notch promotes mature duct development, whereas activation at E15.5 does not affect differentiation.

reflecting the initial differentiation state of *Hes1*$^+$ cells, to that observed after a 2-month 'chase', in which time cells might have adopted new fates. As in the 48-hour chase experiment, we detected acinar, duct and CAC labeling after 7 days, which persists at 2 months (Fig. 5D-G). Scoring the labeling index of each differentiated cell type (n=3-10 mice analyzed per condition) (see Table S2 in the supplementary material), we found that ~1% of acinar cells were EYFP$^+$ at each timepoint [1.4±0.3% (s.e.m.) at 7 days, 1.3±0.3% at 2 months; Fig. 5H]. By contrast, the labeling index of duct cells (defined here as CK19$^+$ epithelial cells not embedded within acini) increased by roughly twofold, from 8.0±0.6% EYFP$^+$ at 7 days to 15.5±0.6% EYFP$^+$ after 2 months (Fig. 5H). This might indicate that *Hes1* marks a subpopulation of proliferating duct cells, consistent with a mitogenic role for Notch in this lineage (Golson et al., 2009). Regarding centroacinar cells specifically, we found a similar labeling index at both timepoints (27.0±2.9% EYFP$^+$ at 7 days, 26.5±0.9% EYFP$^+$ at 2 months). The relative labeling indices of ducts and CACs raises an alternative explanation of why duct labeling increases over time, namely that expansion of the ductal tree is driven by descent from CACs. Although anatomically plausible, this hypothesis requires work beyond the scope of this study.

Unexpectedly, we also detected *Hes1*^{C2}-labeled cells within islets. In islets and throughout the pancreas and other organs, *Hes1*^{C2} labeled numerous endothelial cells (~20% in all experiments) (see Fig. S9 in the supplementary material and data not shown), which we have not analyzed further. With respect to endocrine cells, we did not observe a single *Hes1*^{C2}-labeled β-cell in these experiments, out of over 2000 insulin$^+$ cells scored at each timepoint (see Table S2 and Fig. S9A-B in the supplementary material). We did find rare glucagon$^+$ α-cells marked by *Hes1*^{C2} at both timepoints (3.2±0.4% EYFP$^+$ at 7 days post-TM, 5.7±1.1% at 2 months) (see Fig. S9C-D in the supplementary material), as well as after very short chase periods (12-24 hours post-TM, data not shown). Although the increased α-cell labeling with time is statistically significant (P<0.05), its biological relevance is unclear: it could indicate rare neogenesis

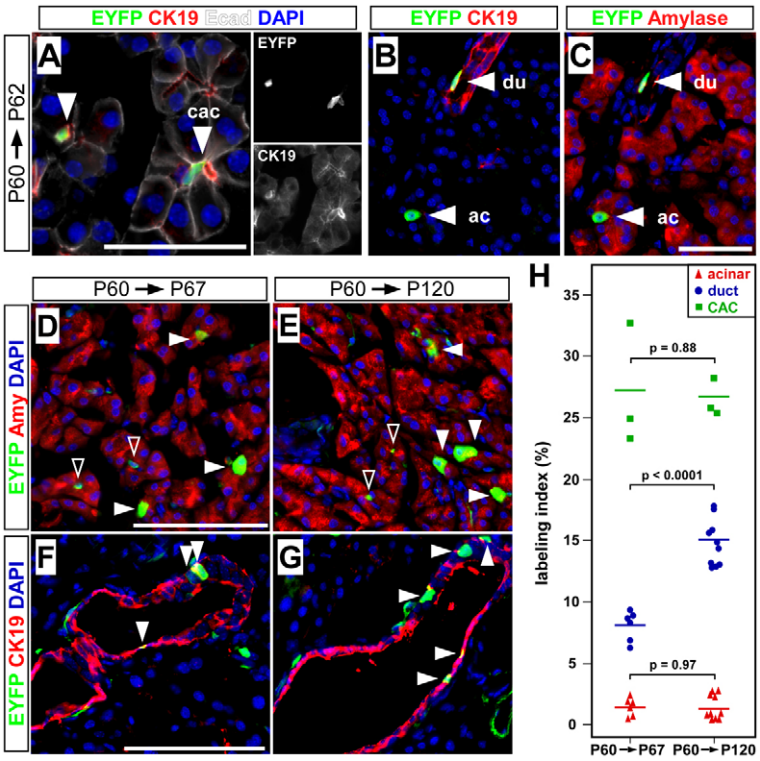

Fig. 5. *Hes1* expression and lineage tracing in the adult exocrine pancreas. Adult (P60) *Hes1*$^{C2/+}$; *R26R*$^{EYFP/+}$ mice were treated with tamoxifen and analyzed for EYFP expression (green) after 2-60 days. (**A**) After short-term labeling, EYFP is expressed by numerous CK19^{+} (red)/E-cadherin^{+} (white) centroacinar cells (cac). Right, single-channel EYFP and CK19 staining. (**B**,**C**) After short-term labeling, EYFP is also detected in CK19^{+} duct (du) cells (B, red) and amylase^{+} acinar (ac) cells (C, red). (**D**,**E**) A similar fraction of labeled acinar (white arrowheads) and centroacinar cells (open arrowheads) is seen after 7- or 60-day chase periods. (**F**,**G**) Between 7 and 60 days post-TM, the fraction of EYFP-labeled duct cells (arrowheads) appears to expand. Scale bars: 50 μm in A-C; 100 μm in D-G. (**H**) Quantifying labeled cells as a fraction of all acinar (red triangles), duct (blue circles) or centroacinar cells (green squares). Each point represents the labeling index of at least five fields from a single pancreas; mean labeling indices (across multiple pancreata) are indicated by horizontal lines. Acinar and CAC labeling does not change over time, whereas that of duct cells increases. *P*-values are determined by Tukey's HSD test.

from the more highly labeled ducts or CACs, although this has not been seen in previous experiments (Kopinke and Murtaugh, 2010; Solar et al., 2009). Alternatively, and consistent with α-cells being labeled at short chase periods, *Hes1* could be expressed by rare α-cells and mark a more proliferative subset of this population. Adult α-cells dynamics have received less attention than those of β-cells, although tools now exist to determine whether significant numbers of adult α-cells are born outside the islet (Thorel et al., 2010).

The lack of β-cell labeling suggests that *Hes1*$^{+}$ cells do not behave as adult precursors for this cell type. Our TM treatment regimen appeared to capture most *Hes1*$^{+}$ cells in the adult pancreas: with respect to centroacinar cells, a higher dose of tamoxifen (3×10 mg, over 3 days) conferred no more labeling than our standard 1×10 mg dose (24.9±0.1% EYFP^{+} at 1 month post-treatment, *n*=2). We propose that *Hes1* expression marks only a subset of CACs in the adult pancreas, which does not contribute to β-cells in vivo.

Independent evidence for the efficiency of adult *Hes1*^{C2} labeling comes from the adult intestine, in which we found that *Hes1*^{C2} does mark stem cells. Low dose (2 mg) tamoxifen treatment of adult (P60) *Hes1*$^{C2/+}$; *R26R*$^{EYFP/+}$ mice (*n*=2) revealed labeling, within 12 hours, of single cells in the crypt base region as well as just above the crypts (Fig. 6A,B). The location of the former cells, representing approx. two-thirds of all EYFP^{+} cells in the intestinal epithelium, agreed with previous *Hes1* expression studies (Jensen et al., 2000; Schroder and Gossler, 2002), whereas the latter may represent transit-amplifying cells in which Notch inhibits secretory lineage specification (Crosnier et al., 2006). After a long-term chase (30 days, *n*=2), we found entire crypt-villus units expressing EYFP, suggesting labeling of intestinal stem cells (Fig. 6C,D). We also found that *Hes1*^{C2}-expressing cells, like bona fide intestinal stem cells (Barker et al., 2009; Sangiorgi and Capecchi, 2008; Zhu et al., 2008), were susceptible to transformation by activated β-catenin [using a *Ctnnb1*$^{lox(ex3)}$ gain-of-function allele (Harada et al., 1999)] (Fig. 6E,F). Importantly, a single 5 mg TM dose was sufficient to label most crypt-villus units along the intestinal tract of *Hes1*$^{C2/+}$; *R26R*$^{LacZ/+}$ mice (*n*=2) after a 6-month chase. Labeling was highest in the duodenum (~90% of crypts), and decreased posteriorly to ~50% labeling in the colon (Fig. 6G-J), frequencies that compare favorably with those of other intestinal stem cell Cre drivers (Barker et al., 2007; Sangiorgi and Capecchi, 2008; Zhu et al., 2008). This high efficiency implies that a 5 mg TM dose was sufficient to recombine most *Hes1*$^{+}$ cells in the intestine; assuming a similar dose-response relationship in the pancreas, our 10 mg TM treatment regimen should also have labeled most *Hes1*$^{+}$ cells in this organ. Taken together, our results highlight the contrasting cellular dynamics of the adult pancreas and intestine, and suggest that *Hes1*^{C2} might be useful to mark and manipulate adult stem cells when they exist in other organs.

Hes1^{CreERT2}-labeled cells do not contribute to β-cells after injury

Although β-cell neogenesis may not be required in the healthy adult pancreas, it might be induced by injury, as in the case of pancreatic duct ligation (PDL) (Inada et al., 2008; Xu et al., 2008). PDL causes inflammation and acinar cell apoptosis distal to the ligation site (Scoggins et al., 2000; Watanabe et al., 1995), which is accompanied by a local increase in β-cell numbers and apparent reappearance of *Neurog3*$^{+}$ β-cell precursors (Wang et al., 1995; Xu et al., 2008). We therefore sought to determine whether *Hes1* marks cells capable of β-cell neogenesis in this model.

Ligation of the dorsal (splenic) pancreas lobe was performed as described by others (Scoggins et al., 2000; Solar et al., 2009; Watanabe et al., 1995; Xu et al., 2008); a full description of our observations in this model will be submitted elsewhere. At 7 days after surgery, acinar cells in the ligated region were completely replaced by fibro-inflammatory cells and epithelial tubules

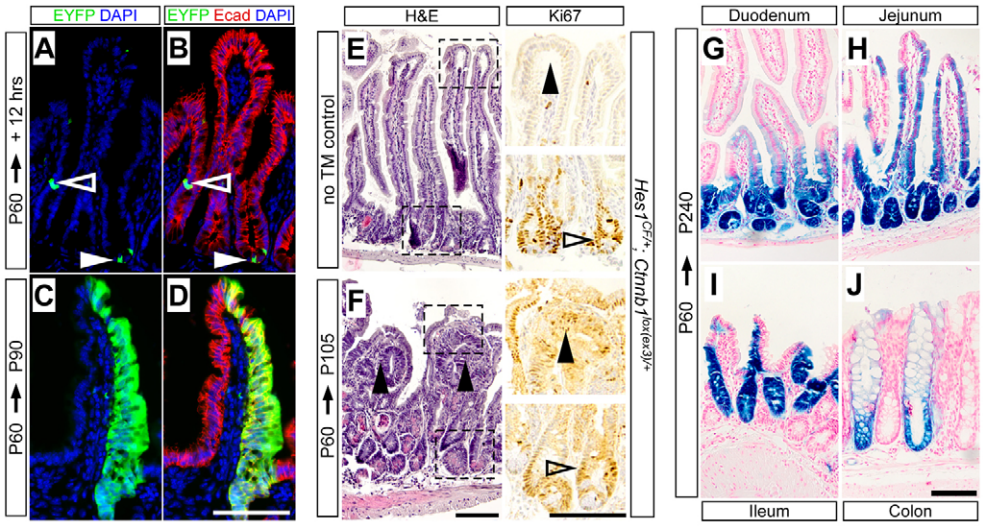

Fig. 6. *Hes1* expression marks intestinal crypt stem cells. (**A-D**) Adult (P60) *Hes1*$^{C2/+}$; *R26R*$^{EYFP/+}$ mice received a single tamoxifen dose, and were stained for labeling of the ileum epithelium (EYFP, green; E-cadherin, red) after 12 hours or 30 days. Short-term labeling (A,B) marks cells in the basal crypt (closed arrowhead) and at the crypt-villus junction (open arrowheads). After a 30-day chase (C,D), labeling encompasses the entire crypt-villus unit, indicating stem cell labeling. (**E**,**F**) P60 *Hes1*$^{C2/+}$; *Ctnnb1*$^{lox(ex3)/+}$ mice were left untreated (E) or administered a single tamoxifen dose (F), and analyzed after 45 days. Hematoxylin and Eosin staining reveals normal morphology of untreated intestine, whereas the small intestines of TM-treated mice exhibit numerous microadenomas (arrowheads) accompanying general tissue disorganization. Outlines indicate areas stained for Ki67 on adjacent sections, which reveal TM-induced expansion of the proliferative compartment from crypts (open arrowheads) to more distal epithelium (closed arrowheads). (**G-J**) *Hes1*$^{C2/+}$; *R26R*$^{LacZ/+}$ mice received a single 5 mg TM dose at P60 and were chased for 180 days before analysis by whole-mount X-gal staining of specific intestinal segments. Uniformly *lacZ*$^{+}$ crypts are detected in all segments, at a decreasing frequency from anterior to posterior. Staining of distal villi was inconsistent (e.g. G) owing to poor penetration of substrate. Scale bars: 100 μm.

(Fig. 7A,B). These epithelia presented suggestive evidence of neogenesis, including association with small β-cell clusters, upregulation of Pdx1, and re-expression of *Neurog3* (Fig. 7E-G and data not shown).

To follow *Hes1*$^{+}$ cells, we administered TM to *Hes1*$^{C2/+}$; *R26R*$^{EYFP/+}$ mice either 1 month pre-surgery (to mark *Hes1*$^{+}$ cells in the healthy pancreas; n=8) or 3 days post-surgery (to capture progenitor-like cells upregulating *Hes1* after injury; n=4), and analyzed EYFP expression 7 days after injury. The 7-day timepoint was chosen for consistency with previous studies indicating a doubling of β-cell mass at this stage, possibly owing to ductal neogenesis (Solar et al., 2009; Wang et al., 1995; Xu et al., 2008). From each mouse, we analyzed 8-10 sections spaced evenly throughout the ligated region (see Fig. S2 in the supplementary material), manually scanning the entire area of each section for EYFP^{+}/insulin^{+} cells (encompassing ~10,000 insulin^{+} cells scanned per ligated pancreas). We did not find a single *Hes1*^{C2}-labeled β-cell in any pancreas, regardless of labeling strategy (Fig. 7C,D and data not shown). We did observe widespread labeling of E-cadherin^{+} and CK19^{+} epithelial complexes in ligated pancreata [~15-20%, a labeling index similar to that of duct and centroacinar cells in the absence of injury (Fig. 5H)], in both TM treatment groups (Fig. 7C,D) (see Table S2 in the supplementary material and data not shown). Although insulin^{+} cells were frequently associated with these complexes, they were always unlabeled (Fig. 7E). These results suggest that *Hes1*^{C2} does not mark cryptic or injury-induced β-cell progenitors in the adult. Although these findings do not exclude the possibility of β-cell differentiation from cultured centroacinar cells in vitro (Rovira et al., 2010), or from *Hes1*-negative cells in vivo, they agree with an independent finding that ducts do not generate β-cells after PDL (Solar et al., 2009).

DISCUSSION

Hes1 is a major Notch target in diverse tissues (Kageyama et al., 2007), and we use its expression as a 'tag' to determine where and when Notch is active in the pancreas. In the embryonic pancreas, our results suggest that early *Hes1*$^{+}$ cells are multipotent progenitors, the differentiation of which is inhibited by Notch, whereas late *Hes1*$^{+}$ cells are exocrine restricted, and respond to elevated Notch levels by becoming ducts (Fig. 3H; Fig. 4F). Our findings in the adult pancreas suggest that *Hes1* expression is restricted to differentiated cells, most abundant within the centroacinar population, and that *Hes1*$^{+}$ cells do not normally behave as cryptic or facultative stem cells for endocrine β-cells. *Hes1*^{C2} provides a novel tool with which to analyze embryonic and adult cells in the pancreas, and our studies of the adult intestine suggest that it might be widely useful in marking and manipulating adult stem cells.

Hes1 lineage and Notch function in the embryonic pancreas

Our results confirm and significantly extend prior studies of Notch-responsive cells in the embryonic pancreas. For example, mapping Notch1 receptor activation in vivo, via *N$_1$IP-Cre*, reveals scattered labeling throughout the exocrine and endocrine pancreas (Vooijs et al., 2007). Although *N$_1$IP-Cre* identifies the range of cell types that had experienced Notch1 signaling at some prior stage, it cannot determine when that signaling occurred. As our CreERT2 approach allowed us to mark cells expressing *Hes1* at specific developmental stages, we could show that most islet-fated cells had received Notch signals only before the 'secondary transition', a wave of endocrine differentiation spanning ~E13.5 to birth in the mouse (Herrera et al., 1991; Pictet and Rutter, 1972).

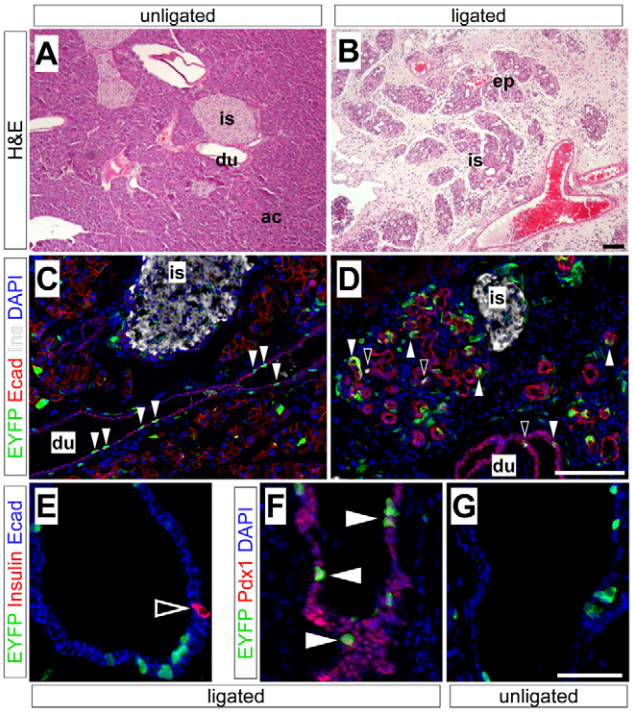

Fig. 7. No detectable β-cell neogenesis from *Hes1*$^{+}$ cells after duct ligation. (**A**,**B**) Hematoxylin and Eosin-stained sections of wild-type pancreata, 7 days after duct ligation, reveals loss of acinar cells (ac) and expansion of epithelial nests (ep) specifically in the ligated region. Islets (is) are preserved. (**C-G**) *Hes1*$^{C2/+}$; *R26R*$^{EYFP/+}$ mice received TM 1 month pre-ligation, and were analyzed 7 days post-ligation by staining for EYFP (green), E-cadherin (C,D, red; E, blue), insulin (C,D, white; E, red) and Pdx1 (F,G, red). In the unligated region (C), the *Hes1* lineage encompasses duct (closed arrowheads), acinar and endothelial cells. In the ligated area (D), labeling is found in epithelial (closed arrowheads) and endothelial cells. Insulin^{+} cells in duct-like structures are unlabeled (D,E, open arrowheads). Pdx1 is upregulated in ligated ducts, including *Hes1*^{C2}-labeled cells (F), but remained undetectable in unligated ducts (G). Scale bars: 100 μm in A-D; 50 μm in E-G.

The fact that Hes1 can directly repress *Neurog3* (Lee et al., 2001), together with the excessive α-cell differentiation observed in *Hes1* mutants (Jensen et al., 2000), might suggest that *Hes1* downregulation is rate-limiting for endocrine specification. However, *Neurog3*$^{+}$ endocrine precursors continue to be generated throughout the secondary transition, with a peak at E15.5 (Gradwohl et al., 2000; Gu et al., 2002), and the majority of β-cells differentiate between E15.5 and birth (Herrera et al., 1991). Our results suggest that these cells must derive from progenitors that turn on *Neurog3* several days after having turned off *Hes1*, arguing that endocrine specification is not immediately induced upon Notch-*Hes1* downregulation. Indeed, the secondary transition appears to proceed normally in *Notch1*/*Notch2* double mutants (Nakhai et al., 2008), suggesting that Notch-independent mechanisms control the timing of *Neurog3* expression and islet differentiation in late embryogenesis.

Prior to the secondary transition, both *Cpa1*$^{+}$ tip cells and *Hnf1b*$^{+}$ ducts contain multipotent progenitors (Solar et al., 2009; Zhou et al., 2007). *Hes1* is expressed in and labels both tip cells and ducts during early pancreas development (see Fig. S3A in the supplementary material and data not shown), suggesting that it marks multipotent progenitors regardless of anatomical location. After E13.5, *Cpa1*$^{+}$ cells behave as acinar-restricted precursors, whereas *Hnf1b*$^{+}$ cells become restricted to islet and duct fates (Solar et al., 2009; Zhou et al., 2007). To reconcile these observations with our hypothesis that *Hes1* marks bipotent acinar/duct progenitors after E13.5, we suggest that acinar-restricted *Cpa1*$^{+}$ cells derive from bipotent *Hes1*$^{+}$ cells from ~E13.5-E15.5. Indeed, analysis of GFP perdurance in *Sox9-EGFP* transgenic embryos suggests that ducts give rise to acini through at least E14 (Seymour et al., 2008). That late duct-to-acinar differentiation was not observed with *Hnf1b-CreERT2* may reflect inefficient labeling by this transgene in utero (Solar et al., 2009), combined with the overall rarity of *Hes1*$^{+}$ progenitors at these stages (Figs 1, 2). In zebrafish, Notch is required for duct specification of exocrine-restricted progenitors (Yee et al., 2005), and our results suggest that Notch also promotes duct development in late mouse embryogenesis.

Hes1 expression and phenotypic plasticity in the adult pancreas

Notch is implicated in self-renewal of adult stem cells (Chiba, 2006), and *Hes1*^{C2} robustly labels stem cells in the intestinal crypts. Under conditions sufficient to label the majority of intestinal stem cells, however, we do not find evidence that *Hes1*^{C2} labels stem-like cells in the adult pancreas. Instead, we find that *Hes1*^{C2} is active in several mature cell types, of which centroacinar cells are the most highly labeled. Previous studies indicate that *Hes1* expression and Notch activity are highest in CACs, and lower in more proximal ductal elements (Miyamoto et al., 2003; Parsons et al., 2009; Stanger et al., 2005), closely paralleling the *Hes1*^{C2} labeling pattern. Although we have not obtained reliable Hes1 immunostaining in adult pancreata (data not shown), *Hes1*^{C2} labeling suggests that it is also expressed by rare differentiated α-cells and acinar cells. Whether Notch has a functional role in these cells remains to be determined. Importantly, we never observe *Hes1*^{C2} labeling of insulin^{+} β-cells, suggesting little or no contribution to these cells from the adult *Hes1* lineage.

This result appears inconsistent with the finding that CACs, isolated based on high aldehyde dehydrogenase activity, can give rise to β-cells and other cell types in vitro (Rovira et al., 2010). Interestingly, however, the cells isolated in that study expressed only low levels of *Hes1*, suggesting that they represent a distinct subpopulation of CACs. Indeed, we find that only approx. one-quarter of CACs are labeled by *Hes1*^{C2} using our standard tamoxifen dose, and that this proportion is not increased by a threefold higher dose. Our results therefore constitute in vivo evidence for heterogeneity within the duct and CAC compartments, and suggest that the *Hes1*$^{+}$ subpopulation does not normally give rise to β-cells.

Alternatively, the failure of *Hes1*^{C2} to label β-cells might reflect limitations imposed by the micro-environment of the mature pancreas, e.g. active Notch signaling reinforcing ductal fate, which could be removed in tissue culture or during regeneration. To address this, we adopted an injury model, pancreatic duct ligation, which has provided suggestive evidence of β-cell neogenesis from ductal progenitors (Wang et al., 1995; Xu et al., 2008). In rats and mice, PDL is reported to lead to a local doubling of β-cell mass within 1 week (Wang et al., 1995; Xu et al., 2008), together with inflammation, acinar cell apoptosis and ductal hyperplasia (Scoggins et al., 2000; Watanabe et al., 1995). At 7 days post-PDL, we find that *Hes1*^{C2}-labeled cells contribute to the abnormal ductal epithelium, but

not to β-cells located either in islets or within or near ducts. We note that identical results were obtained using *Hnf1b-CreERT2*, which labels cells throughout the ductal network (Solar et al., 2009), suggesting that new β-cells arise after PDL either from pre-existing β-cells, or from a duct subpopulation that expresses neither *Hnf1b* nor *Hes1* (Inada et al., 2008).

Our results do not exclude the possibility that CACs or other *Hes1*$^{+}$ cells could give rise to β-cells more than 7 days post-PDL, although further increases in β-cell mass beyond this timepoint have not been reported (Wang et al., 1995; Xu et al., 2008), and adipocyte infiltration at later stages may produce secondary effects on islets (Watanabe et al., 1995). It is also possible that other injury models might evoke β-cell differentiation from *Hes1*$^{+}$ cells, much as glucagon^{+} α-cells can transform into β-cells after extreme β-cell loss, despite an otherwise absolute barrier to interconversion (Thorel et al., 2010). We also note that, as *Hes1*^{C2} labels a minority of CACs, our study does not definitively test CAC differentiation potential. Several other CreERT drivers, particularly those with stringent tamoxifen dependence, have been shown to recombine only a minority of their putative target cells (Desai et al., 2007; Dor et al., 2004; Solar et al., 2009), raising the possibility of unlabeled subpopulations. Our results, however, suggest that *Hes1*^{C2} does label most *Hes1*$^{+}$ cells in the adult, but that *Hes1*$^{+}$ duct and centroacinar cells cannot generate β-cells under the conditions studied here. In sum, *Hes1*^{C2} provides a new tool to test the role of Notch-responsive cells in physiological and pathological conditions, and our studies raise the issue of whether Notch activity functionally subdivides pancreatic duct cells into those with and without progenitor-like potential.

Acknowledgements

We thank Nadean Brown (University of Cincinnati) for the Hes1 antibody, Makoto Mark Taketo (Kyoto University) for *Ctnnb1*$^{lox(ex3)}$ mice, and Kirk Thomas and Mario Capecchi (University of Utah) for reagents and advice on gene targeting. We thank Richard Dorsky, Edward Levine and Nadja Makki for helpful comments on this manuscript. This work was supported by grants from the Searle Scholars Foundation (06-B-116), NIH (R01-DK075072) and Beta Cell Biology Consortium (U01-DK072473, subaward VUMC35146) to L.C.M., and a Boehringer Ingelheim Fonds graduate fellowship to D.K. Deposited in PMC for release after 12 months.

Competing interests statement

The authors declare no competing financial interests.

Supplementary material

Supplementary material for this article is available at
http://dev.biologists.org/lookup/suppl/doi:10.1242/dev.053843/-/DC1

References

Antoniou, A., Raynaud, P., Cordi, S., Zong, Y., Tronche, F., Stanger, B. Z., Jacquemin, P., Pierreux, C. E., Clotman, F. and Lemaigre, F. P. (2009). Intrahepatic bile ducts develop according to a new mode of tubulogenesis regulated by the transcription factor SOX9. *Gastroenterology* **136**, 2325-2333.

Apelqvist, A., Li, H., Sommer, L., Beatus, P., Anderson, D. J., Honjo, T., Hrabe de Angelis, M., Lendahl, U. and Edlund, H. (1999). Notch signalling controls pancreatic cell differentiation. *Nature* **400**, 877-881.

Barker, N., van Es, J. H., Kuipers, J., Kujala, P., van den Born, M., Cozijnsen, M., Haegebarth, A., Korving, J., Begthel, H., Peters, P. J. et al. (2007). Identification of stem cells in small intestine and colon by marker gene Lgr5. *Nature* **449**, 1003-1007.

Barker, N., Ridgway, R. A., van Es, J. H., van de Wetering, M., Begthel, H., van den Born, M., Danenberg, E., Clarke, A. R., Sansom, O. J. and Clevers, H. (2009). Crypt stem cells as the cells-of-origin of intestinal cancer. *Nature* **457**, 608-611.

Chiba, S. (2006). Notch signaling in stem cell systems. *Stem Cells* **24**, 2437-2447.

Crosnier, C., Stamataki, D. and Lewis, J. (2006). Organizing cell renewal in the intestine: stem cells, signals and combinatorial control. *Nat. Rev. Genet.* **7**, 349-359.

De La O, J. P., Emerson, L. L., Goodman, J. L., Froebe, S. C., Illum, B. E., Curtis, A. B. and Murtaugh, L. C. (2008). Notch and Kras reprogram pancreatic acinar cells to ductal intraepithelial neoplasia. *Proc. Natl. Acad. Sci. USA* **105**, 18907-18912.

Desai, B. M., Oliver-Krasinski, J., De Leon, D. D., Farzad, C., Hong, N., Leach, S. D. and Stoffers, D. A. (2007). Preexisting pancreatic acinar cells contribute to acinar cell, but not islet beta cell, regeneration. *J. Clin. Invest.* **117**, 971-977.

Dor, Y., Brown, J., Martinez, O. I. and Melton, D. A. (2004). Adult pancreatic beta-cells are formed by self-duplication rather than stem-cell differentiation. *Nature* **429**, 41-46.

Dovey, H. F., John, V., Anderson, J. P., Chen, L. Z., de Saint Andrieu, P., Fang, L. Y., Freedman, S. B., Folmer, B., Goldbach, E., Holsztynska, E. J. et al. (2001). Functional gamma-secretase inhibitors reduce beta-amyloid peptide levels in brain. *J. Neurochem.* **76**, 173-181.

Esni, F., Ghosh, B., Biankin, A. V., Lin, J. W., Albert, M. A., Yu, X., MacDonald, R. J., Civin, C. I., Real, F. X., Pack, M. A. et al. (2004). Notch inhibits Ptf1 function and acinar cell differentiation in developing mouse and zebrafish pancreas. *Development* **131**, 4213-4224.

Farley, F. W., Soriano, P., Steffen, L. S. and Dymecki, S. M. (2000). Widespread recombinase expression using FLPeR (flipper) mice. *Genesis* **28**, 106-110.

Feil, R., Wagner, J., Metzger, D. and Chambon, P. (1997). Regulation of Cre recombinase activity by mutated estrogen receptor ligand-binding domains. *Biochem. Biophys. Res. Commun.* **237**, 752-757.

Geisler, F., Nagl, F., Mazur, P. K., Lee, M., Zimber-Strobl, U., Strobl, L. J., Radtke, F., Schmid, R. M. and Siveke, J. T. (2008). Liver-specific inactivation of Notch2, but not Notch1, compromises intrahepatic bile duct development in mice. *Hepatology* **48**, 607-616.

Gittes, G. K. (2009). Developmental biology of the pancreas: a comprehensive review. *Dev. Biol.* **326**, 4-35.

Golson, M. L., Loomes, K. M., Oakey, R. and Kaestner, K. H. (2009). Ductal malformation and pancreatitis in mice caused by conditional Jag1 deletion. *Gastroenterology* **136**, 1761-1771.

Gradwohl, G., Dierich, A., LeMeur, M. and Guillemot, F. (2000). neurogenin3 is required for the development of the four endocrine cell lineages of the pancreas. *Proc. Natl. Acad. Sci. USA* **97**, 1607-1611.

Greenwood, A. L., Li, S., Jones, K. and Melton, D. A. (2007). Notch signaling reveals developmental plasticity of Pax4(+) pancreatic endocrine progenitors and shunts them to a duct fate. *Mech. Dev.* **124**, 97-107.

Gu, G., Dubauskaite, J. and Melton, D. A. (2002). Direct evidence for the pancreatic lineage: NGN3+ cells are islet progenitors and are distinct from duct progenitors. *Development* **129**, 2447-2457.

Hald, J., Hjorth, J. P., German, M. S., Madsen, O. D., Serup, P. and Jensen, J. (2003). Activated Notch1 prevents differentiation of pancreatic acinar cells and attenuate endocrine development. *Dev. Biol.* **260**, 426-437.

Harada, N., Tamai, Y., Ishikawa, T., Sauer, B., Takaku, K., Oshima, M. and Taketo, M. M. (1999). Intestinal polyposis in mice with a dominant stable mutation of the beta-catenin gene. *EMBO J.* **18**, 5931-5942.

Hayashi, K. Y., Tamaki, H., Handa, K., Takahashi, T., Kakita, A. and Yamashina, S. (2003). Differentiation and proliferation of endocrine cells in the regenerating rat pancreas after 90% pancreatectomy. *Arch. Histol. Cytol.* **66**, 163-174.

Herrera, P. L., Huarte, J., Sanvito, F., Meda, P., Orci, L. and Vassalli, J. D. (1991). Embryogenesis of the murine endocrine pancreas; early expression of pancreatic polypeptide gene. *Development* **113**, 1257-1265.

Inada, A., Nienaber, C., Katsuta, H., Fujitani, Y., Levine, J., Morita, R., Sharma, A. and Bonner-Weir, S. (2008). Carbonic anhydrase II-positive pancreatic cells are progenitors for both endocrine and exocrine pancreas after birth. *Proc. Natl. Acad. Sci. USA* **105**, 19915-19919.

Ishibashi, M., Ang, S. L., Shiota, K., Nakanishi, S., Kageyama, R. and Guillemot, F. (1995). Targeted disruption of mammalian hairy and Enhancer of split homolog-1 (HES-1) leads to up-regulation of neural helix-loop-helix factors, premature neurogenesis, and severe neural tube defects. *Genes Dev.* **9**, 3136-3148.

Jensen, J., Pedersen, E. E., Galante, P., Hald, J., Heller, R. S., Ishibashi, M., Kageyama, R., Guillemot, F., Serup, P. and Madsen, O. D. (2000). Control of endodermal endocrine development by Hes-1. *Nat. Genet.* **24**, 36-44.

Kageyama, R., Ohtsuka, T. and Kobayashi, T. (2007). The Hes gene family: repressors and oscillators that orchestrate embryogenesis. *Development* **134**, 1243-1251.

Kobayashi, H., Spilde, T. L., Li, Z., Marosky, J. K., Bhatia, A. M., Hembree, M. J., Prasadan, K., Preuett, B. L. and Gittes, G. K. (2002). Lectin as a marker for staining and purification of embryonic pancreatic epithelium. *Biochem. Biophys. Res. Commun.* **293**, 691-697.

Kodama, Y., Hijikata, M., Kageyama, R., Shimotohno, K. and Chiba, T. (2004). The role of notch signaling in the development of intrahepatic bile ducts. *Gastroenterology* **127**, 1775-1786.

Kopinke, D. and Murtaugh, L. C. (2010). Exocrine-to-endocrine differentiation is detectable only prior to birth in the uninjured mouse pancreas. *BMC Dev. Biol.* **10**, 38.

Lai, E. C. (2004). Notch signaling: control of cell communication and cell fate. *Development* **131**, 965-973.
Lammert, E., Brown, J. and Melton, D. A. (2000). Notch gene expression during pancreatic organogenesis. *Mech. Dev.* **94**, 199-203.
Lee, J. C., Smith, S. B., Watada, H., Lin, J., Scheel, D., Wang, J., Mirmira, R. G. and German, M. S. (2001). Regulation of the pancreatic pro-endocrine gene neurogenin3. *Diabetes* **50**, 928-936.
Liu, P., Jenkins, N. A. and Copeland, N. G. (2003). A highly efficient recombineering-based method for generating conditional knockout mutations. *Genome Res.* **13**, 476-484.
Lozier, J., McCright, B. and Gridley, T. (2008). Notch signaling regulates bile duct morphogenesis in mice. *PLoS ONE* **3**, e1851.
Miyamoto, Y., Maitra, A., Ghosh, B., Zechner, U., Argani, P., Iacobuzio-Donahue, C. A., Sriuranpong, V., Iso, T., Meszoely, I. M., Wolfe, M. S. et al. (2003). Notch mediates TGF alpha-induced changes in epithelial differentiation during pancreatic tumorigenesis. *Cancer Cell* **3**, 565-576.
Murtaugh, L. C., Stanger, B. Z., Kwan, K. M. and Melton, D. A. (2003). Notch signaling controls multiple steps of pancreatic differentiation. *Proc. Natl. Acad. Sci. USA* **100**, 14920-14925.
Murtaugh, L. C., Law, A. C., Dor, Y. and Melton, D. A. (2005). Beta-Catenin is essential for pancreatic acinar but not islet development. *Development* **132**, 4663-4674.
Nagasao, J., Yoshioka, K., Amasaki, H. and Mutoh, K. (2003). Centroacinar and intercalated duct cells as potential precursors of pancreatic endocrine cells in rats treated with streptozotocin. *Ann. Anat.* **185**, 211-216.
Nagy, A., Rossant, J., Nagy, R., Abramow-Newerly, W. and Roder, J. C. (1993). Derivation of completely cell culture-derived mice from early-passage embryonic stem cells. *Proc. Natl. Acad. Sci. USA* **90**, 8424-8428.
Nakhai, H., Siveke, J. T., Klein, B., Mendoza-Torres, L., Mazur, P. K., Algul, H., Radtke, F., Strobl, L., Zimber-Strobl, U. and Schmid, R. M. (2008). Conditional ablation of Notch signaling in pancreatic development. *Development* **135**, 2757-2765.
Parsons, M. J., Pisharath, H., Yusuff, S., Moore, J. C., Siekmann, A. F., Lawson, N. and Leach, S. D. (2009). Notch-responsive cells initiate the secondary transition in larval zebrafish pancreas. *Mech. Dev.* **126**, 898-912.
Pictet, R. and Rutter, W. J. (1972). Development of the embryonic endocrine pancreas. In *Handbook of Physiology, Section 7*, vol. 1 (ed. D. Steiner and N. Freinkel), pp. 25-66. Baltimore: Williams & Williams.
Rovira, M., Scott, S. G., Liss, A. S., Jensen, J., Thayer, S. P. and Leach, S. D. (2010). Isolation and characterization of centroacinar/terminal ductal progenitor cells in adult mouse pancreas. *Proc. Natl. Acad. Sci. USA* **107**, 75-80.
Sangiorgi, E. and Capecchi, M. R. (2008). Bmi1 is expressed in vivo in intestinal stem cells. *Nat. Genet.* **40**, 915-920.
Schroder, N. and Gossler, A. (2002). Expression of Notch pathway components in fetal and adult mouse small intestine. *Gene Expr. Patterns* **2**, 247-250.
Scoggins, C. R., Meszoely, I. M., Wada, M., Means, A. L., Yang, L. and Leach, S. D. (2000). p53-dependent acinar cell apoptosis triggers epithelial proliferation in duct-ligated murine pancreas. *Am. J. Physiol. Gastrointest. Liver Physiol.* **279**, G827-G836.
Seymour, P. A., Freude, K. K., Dubois, C. L., Shih, H. P., Patel, N. A. and Sander, M. (2008). A dosage-dependent requirement for Sox9 in pancreatic endocrine cell formation. *Dev. Biol.* **323**, 19-30.
Solar, M., Cardalda, C., Houbracken, I., Martin, M., Maestro, M. A., De Medts, N., Xu, X., Grau, V., Heimberg, H., Bouwens, L. et al. (2009). Pancreatic exocrine duct cells give rise to insulin-producing beta cells during embryogenesis but not after birth. *Dev. Cell* **17**, 849-860.
Soriano, P. (1999). Generalized lacZ expression with the ROSA26 Cre reporter strain. *Nat. Genet.* **21**, 70-71.
Srinivas, S., Watanabe, T., Lin, C. S., William, C. M., Tanabe, Y., Jessell, T. M. and Costantini, F. (2001). Cre reporter strains produced by targeted insertion of EYFP and ECFP into the ROSA26 locus. *BMC Dev. Biol.* **1**, 4.
Stanger, B. Z., Stiles, B., Lauwers, G. Y., Bardeesy, N., Mendoza, M., Wang, Y., Greenwood, A., Cheng, K. H., McLaughlin, M., Brown, D. et al. (2005). Pten constrains centroacinar cell expansion and malignant transformation in the pancreas. *Cancer Cell* **8**, 185-195.
Thorel, F., Nepote, V., Avril, I., Kohno, K., Desgraz, R., Chera, S. and Herrera, P. L. (2010). Conversion of adult pancreatic alpha-cells to beta-cells after extreme beta-cell loss. *Nature* **464**, 1149-1154.
Vooijs, M., Ong, C. T., Hadland, B., Huppert, S., Liu, Z., Korving, J., van den Born, M., Stappenbeck, T., Wu, Y., Clevers, H. et al. (2007). Mapping the consequence of Notch1 proteolysis in vivo with NIP-CRE. *Development* **134**, 535-544.
Wang, R. N., Kloppel, G. and Bouwens, L. (1995). Duct- to islet-cell differentiation and islet growth in the pancreas of duct-ligated adult rats. *Diabetologia* **38**, 1405-1411.
Watanabe, S., Abe, K., Anbo, Y. and Katoh, H. (1995). Changes in the mouse exocrine pancreas after pancreatic duct ligation: a qualitative and quantitative histological study. *Arch. Histol. Cytol.* **58**, 365-374.
Xu, X., D'Hoker, J., Stange, G., Bonne, S., De Leu, N., Xiao, X., Van de Casteele, M., Mellitzer, G., Ling, Z., Pipeleers, D. et al. (2008). Beta cells can be generated from endogenous progenitors in injured adult mouse pancreas. *Cell* **132**, 197-207.
Yee, N. S., Lorent, K. and Pack, M. (2005). Exocrine pancreas development in zebrafish. *Dev. Biol.* **284**, 84-101.
Zecchin, E., Filippi, A., Biemar, F., Tiso, N., Pauls, S., Ellertsdottir, E., Gnugge, L., Bortolussi, M., Driever, W. and Argenton, F. (2006). Distinct delta and jagged genes control sequential segregation of pancreatic cell types from precursor pools in zebrafish. *Dev. Biol.* **301**, 192-204.
Zhou, Q., Law, A. C., Rajagopal, J., Anderson, W. J., Gray, P. A. and Melton, D. A. (2007). A multipotent progenitor domain guides pancreatic organogenesis. *Dev. Cell* **13**, 103-114.
Zhu, L., Gibson, P., Currle, D. S., Tong, Y., Richardson, R. J., Bayazitov, I. T., Poppleton, H., Zakharenko, S., Ellison, D. W. and Gilbertson, R. J. (2008). Prominin 1 marks intestinal stem cells that are susceptible to neoplastic transformation. *Nature* **457**, 603-607.
Zong, Y., Panikkar, A., Xu, J., Antoniou, A., Raynaud, P., Lemaigre, F. and Stanger, B. Z. (2009). Notch signaling controls liver development by regulating biliary differentiation. *Development* **136**, 1727-1739.

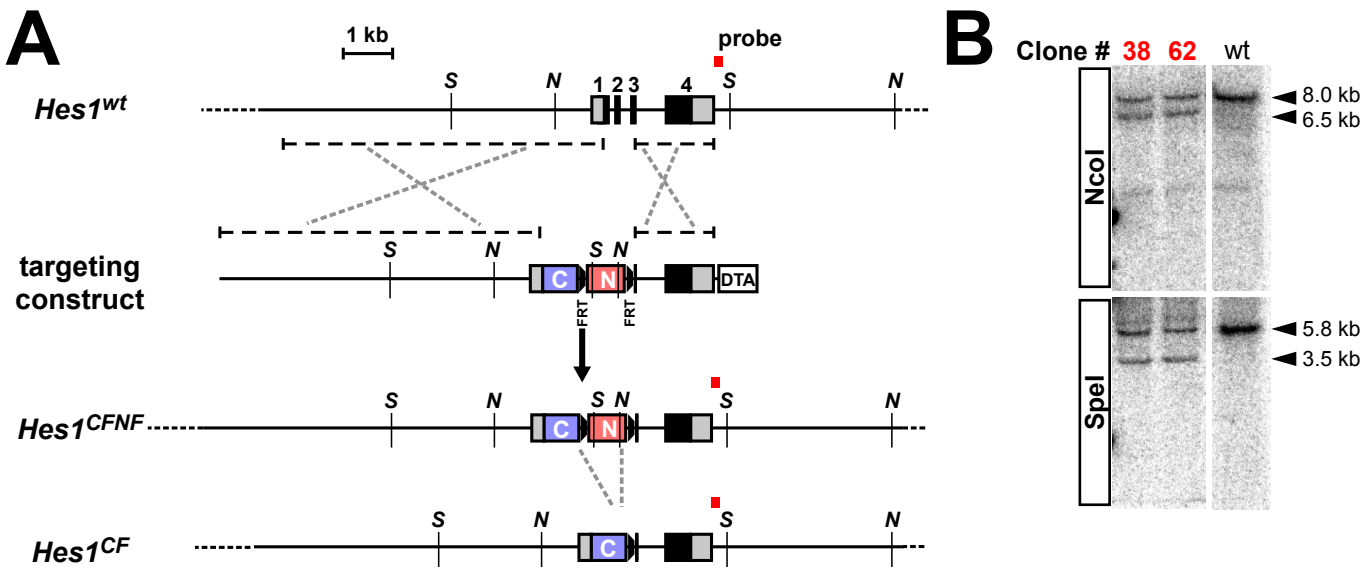
A
1 kb
probe
Hes1wt
S
N
1 2 3
4
S
N
targeting construct
S
N
S N
C
N
DTA
FRT
FRT
Hes1CFNF
S
N
S N
C
N
S
N
Hes1CF
S
N
C
S
N
B
Clone # 38 62 wt
NcoI
8.0 kb
6.5 kb
SpeI
5.8 kb
3.5 kb

Table S1. Cell counts for analyses of embryonic lineage distribution

Experiment	Timepoint	Markers scored	Number of embryos	Number of fields/embryo	Total number of lineage* cells scored
Fig. 3 (*R26R*^{LacZ})	E9.5	Insulin	5	5-10	5405
		Glucagon			6229
		Amylase			5161
		DBA			5985
	E11.5	Insulin	5	5-10	3019
		Glucagon			3035
		Amylase			3572
		DBA			3588
	E13.5	Insulin	3	5-10	1697
		Glucagon			2824
		Amylase			1697
		DBA			2824
	E15.5	Insulin	3	5-10	1084
		Glucagon			894
		Amylase			1084
		DBA			894
Fig. 4 (*Rosa26*^{NIC})	E13.5	Amylase	3	4-6	326
		DBA			326
	E15.5	Amylase	3	4-6	210
		DBA			210

For each figure, we list the number of embryos analyzed per timepoint, the number of microscopic fields scored per embryo and the total number of *lineage marker-expressing cells (across all embryos) scored for co-expression of the indicated differentiation markers.

Table S2. Cell counts for calculations of adult labeling indices

Experiment	Timepoint	Markers scored	Number of mice	Number of fields/mouse	Total number of marker* cells scored
Fig. 5	7-day chase	Amylase	6	7-9	23252
		CK19			4174
	2-month chase	Amylase	10	4-7	25445
		CK19			4167
	7-day chase	CK19$^+$ CAC	3	5-6	336
	2-month chase				222
Fig. 7	7 days post	CK19	5	5-6	8762
		E-cadherin			9603
Fig. S9	7-day chase	Glucagon	6	5-8	2205
		Insulin	3	4-7	2002
	2-month chase	Glucagon	4	5-7	1167
		Insulin	3	5-9	2216

For each figure, we list the number of adult mice analyzed per timepoint, the number of microscopic fields scored per mouse and the total number of *differentiation marker-expressing cells (across all mice) scored for co-expression of the *R26R*^{EYFP} lineage marker. Note that for the duct ligation experiments (Fig. 7), we manually scanned the entire surface of each slide for labeling of insulin$^+$ cells, using the specimens scored here for labeling of CK19$^+$ and E-cadherin$^+$ cells, as well as additional specimens in which CK19$^+$ and E-cadherin$^+$ cells were not analyzed.

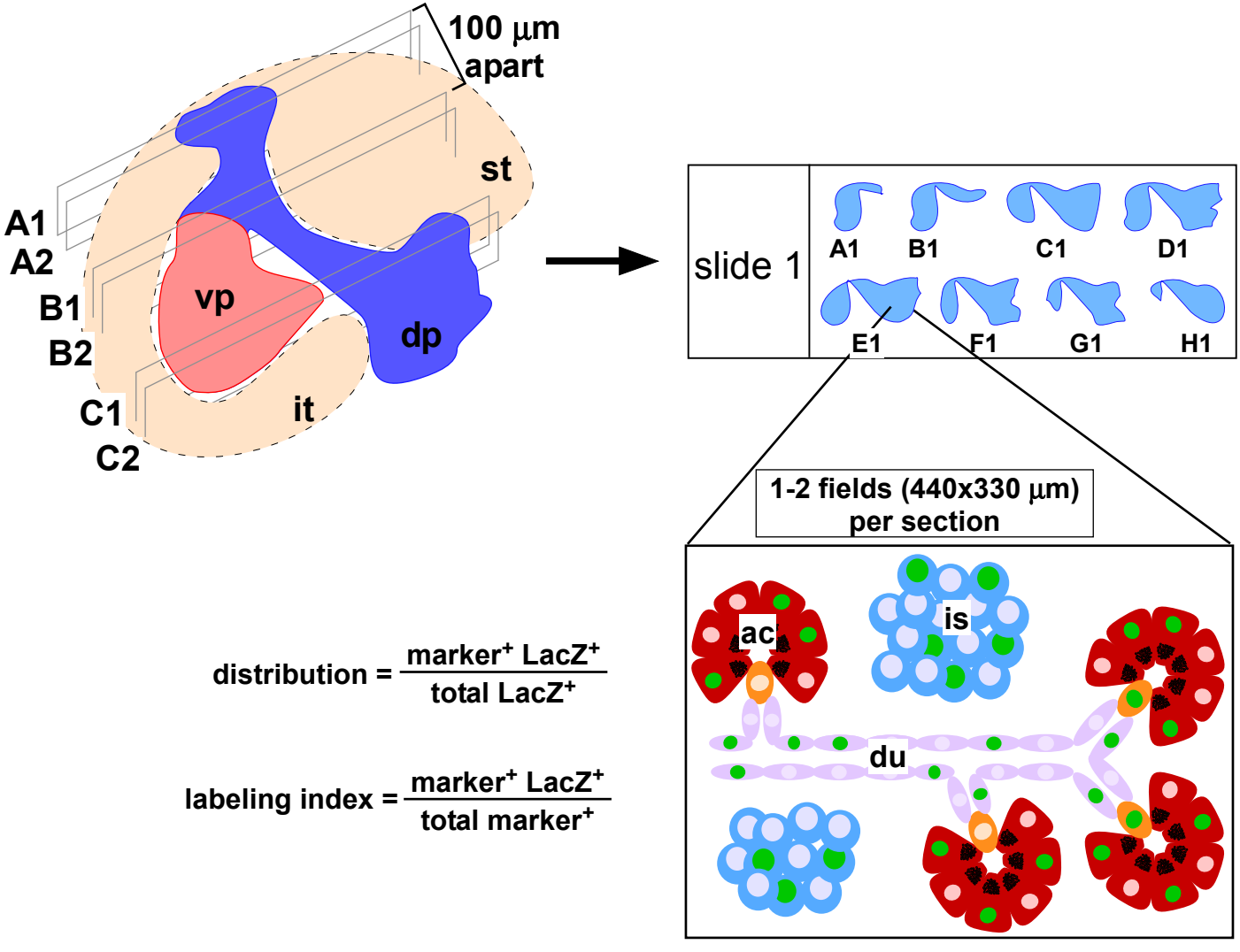
100 µm
apart
st
A1
A2
B1
B2
vp
dp
C1
C2
it
slide 1
A1
B1
C1
D1
E1
F1
G1
H1
1-2 fields (440x330 µm)
per section
ac
is
du
distribution = marker+ LacZ+ / total LacZ+
labeling index = marker+ LacZ+ / total marker+

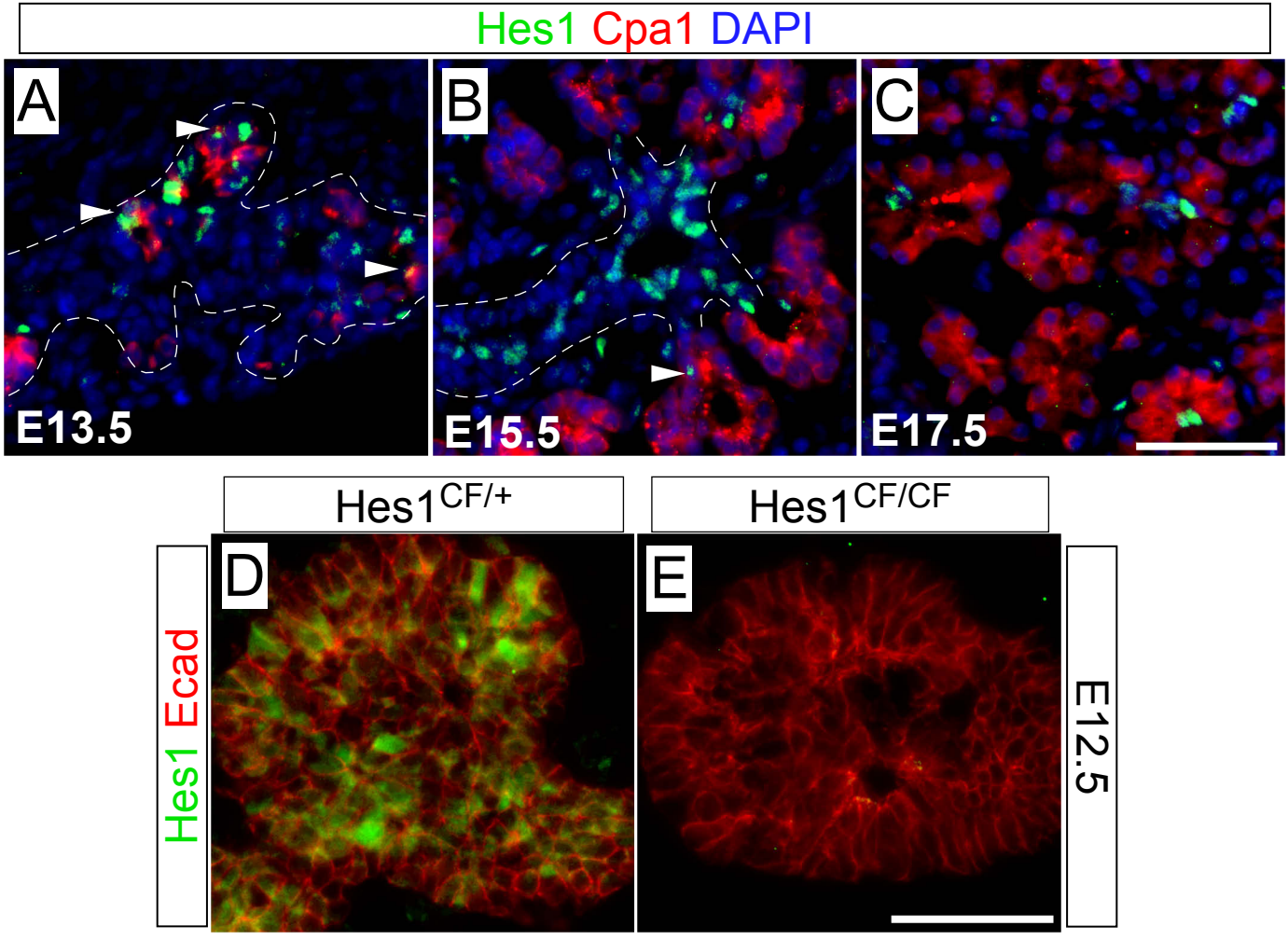
Hes1 Cpa1 DAPI
A
B
C
E13.5
E15.5
E17.5
Hes1CF/+
Hes1CF/CF
D
E
Hes1 Ecad
E12.5

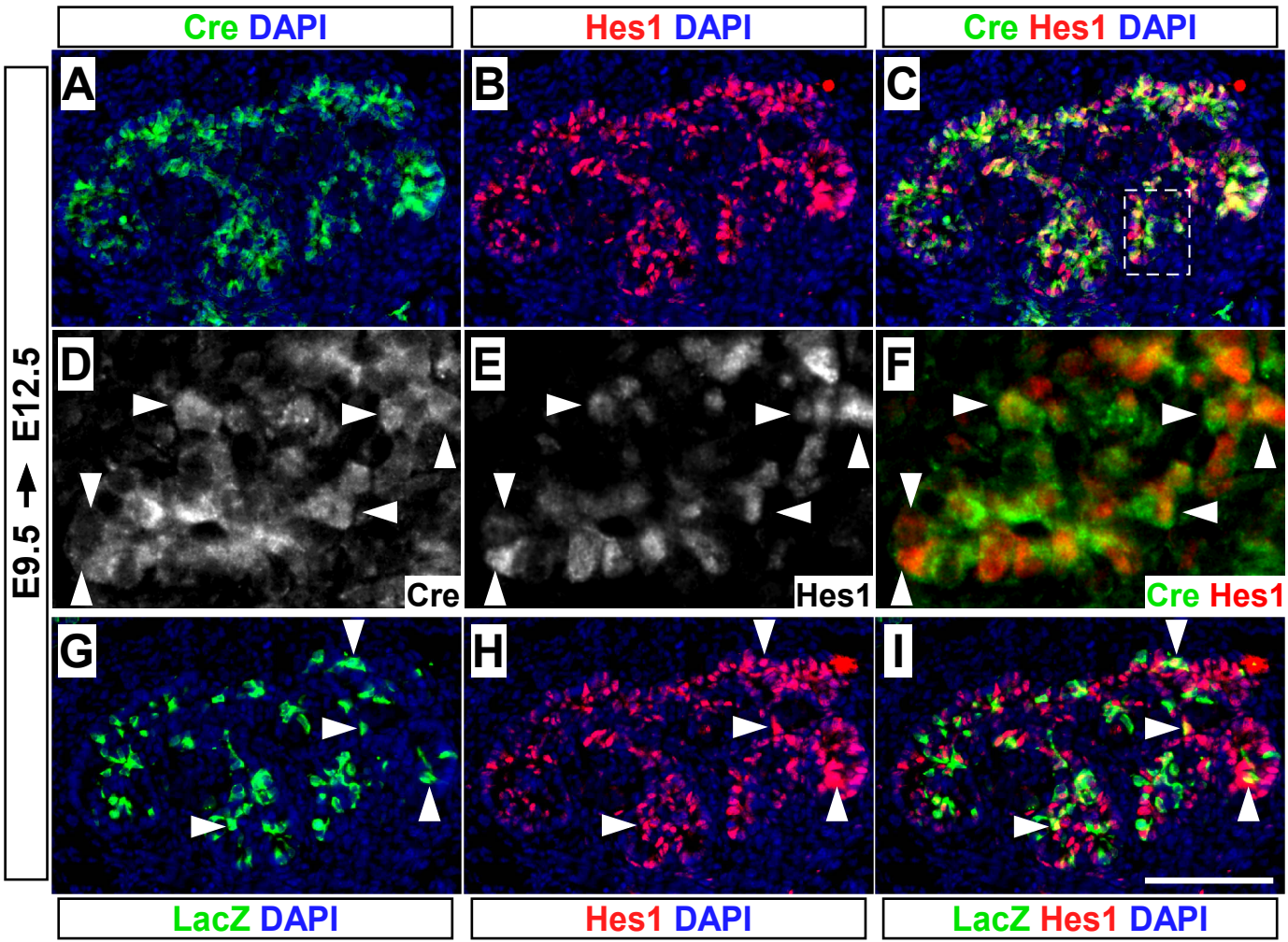
Cre DAPI
Hes1 DAPI
Cre Hes1 DAPI
A
B
C
D
E
F
E9.5 → E12.5
Cre
Hes1
Cre Hes1
G
H
I
LacZ DAPI
Hes1 DAPI
LacZ Hes1 DAPI

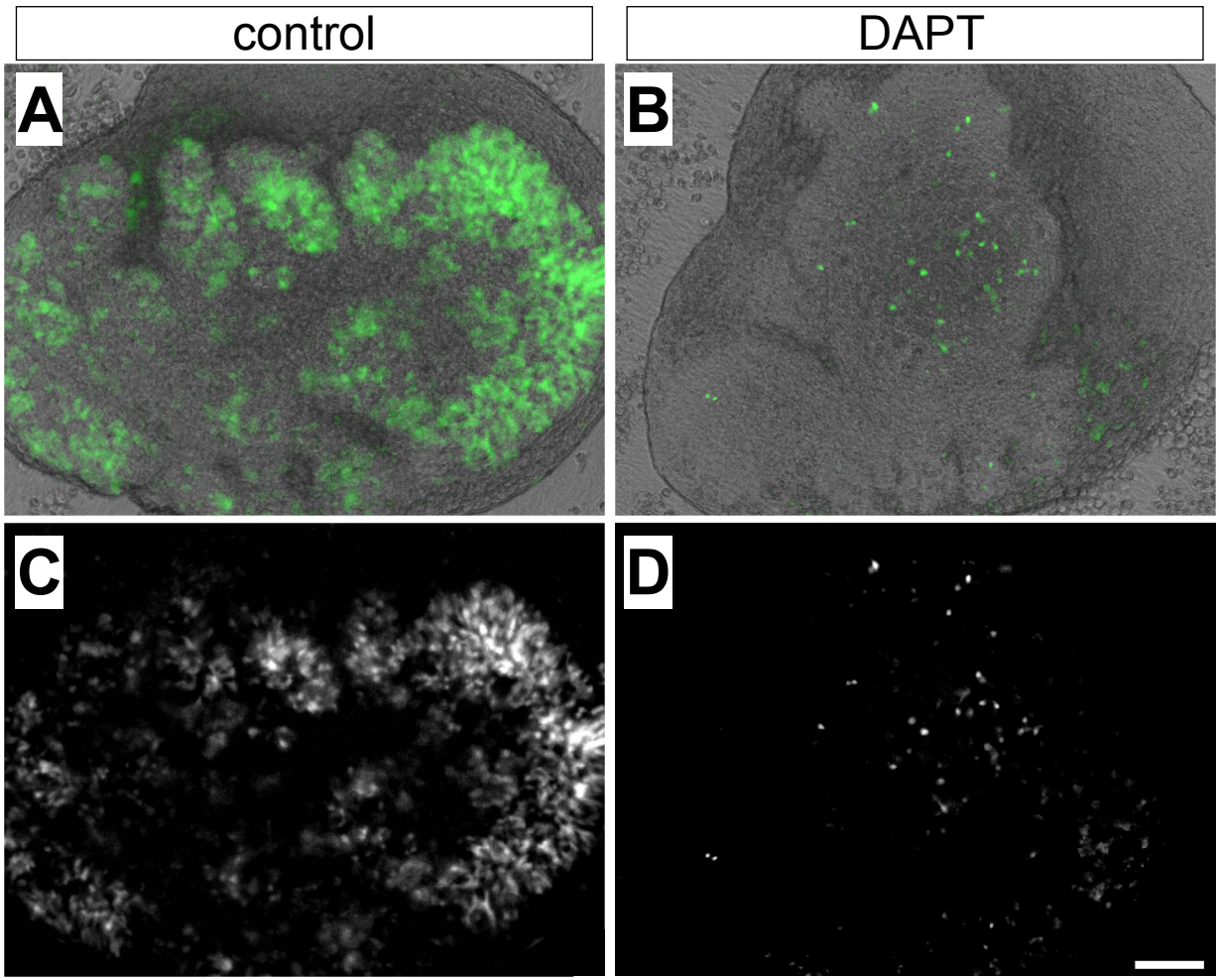
control
DAPT
A
B
C
D

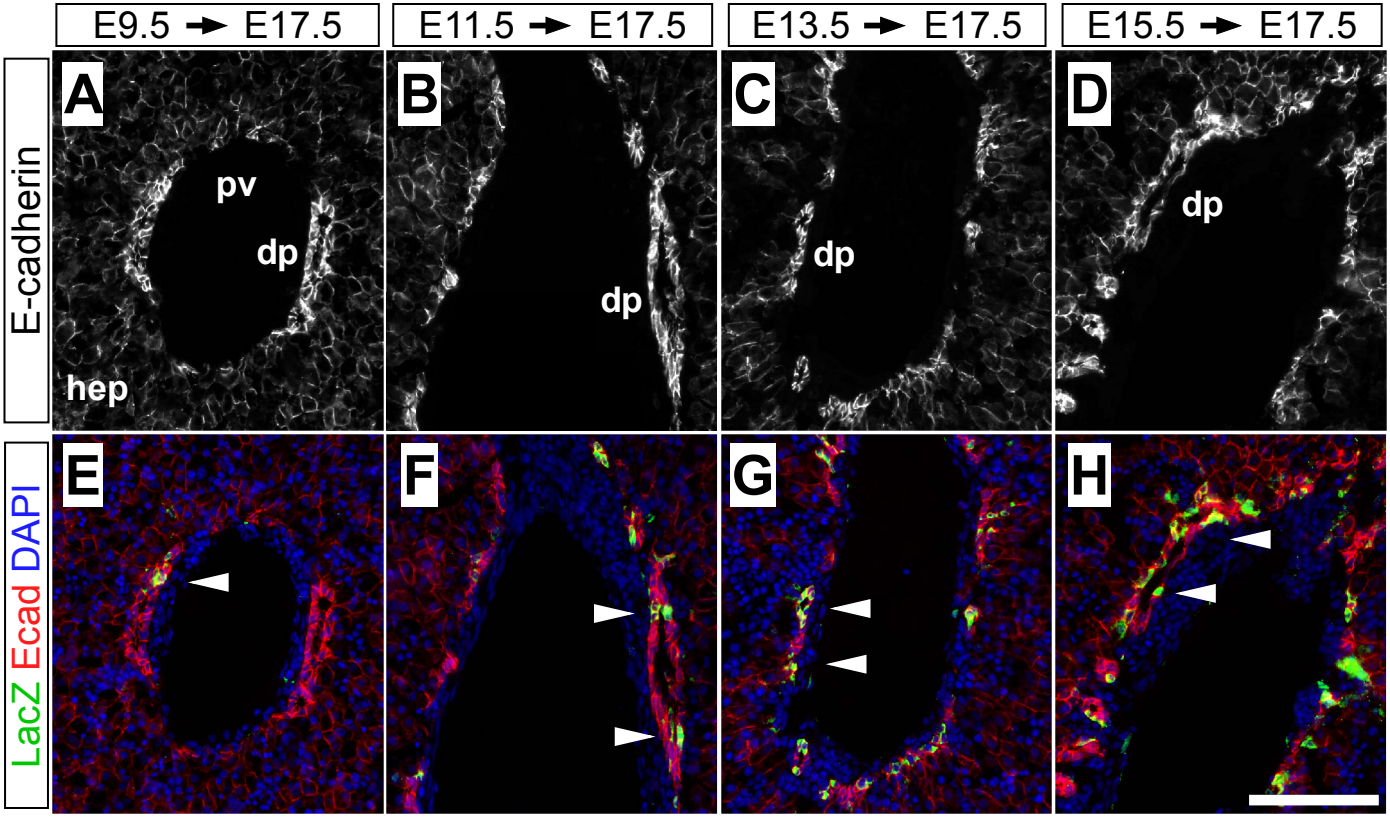
E9.5 → E17.5
E11.5 → E17.5
E13.5 → E17.5
E15.5 → E17.5
E-cadherin
A
B
C
D
pv
dp
hep
dp
dp
dp
LacZ Ecad DAPI
E
F
G
H

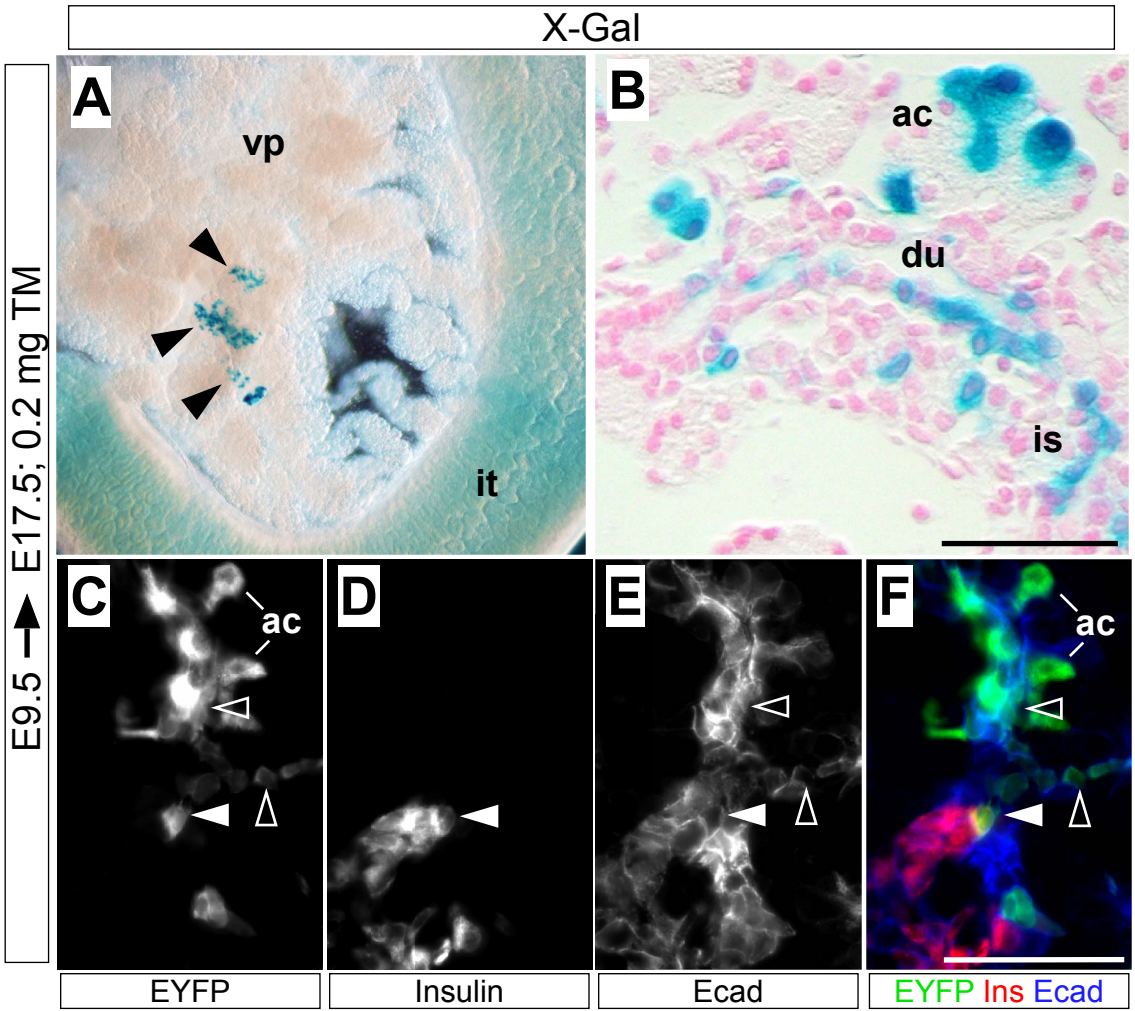
X-Gal
A
vp
it
B
ac
du
is
E9.5 → E17.5; 0.2 mg TM
C
ac
D
E
F
ac
EYFP
Insulin
Ecad
EYFP Ins Ecad

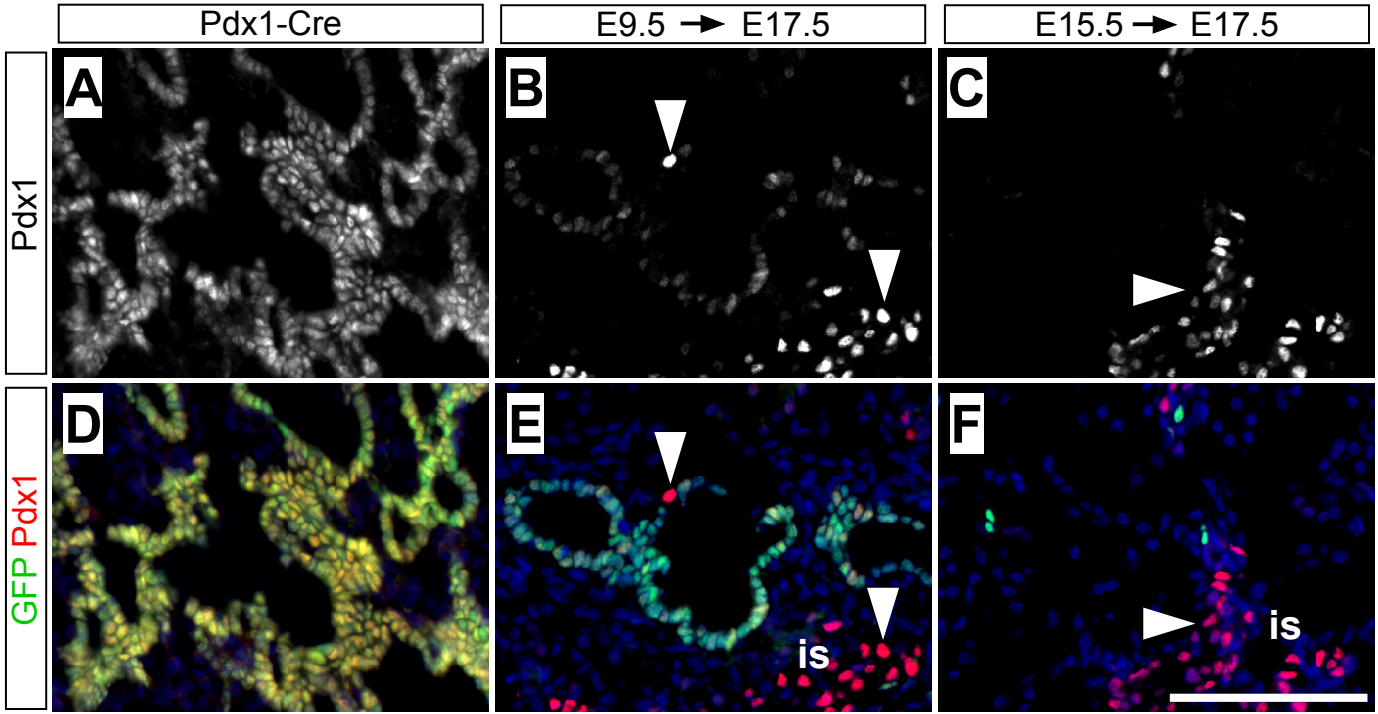
Pdx1-Cre
E9.5 → E17.5
E15.5 → E17.5
Pdx1
GFP Pdx1
A
B
C
D
E
F
is
is

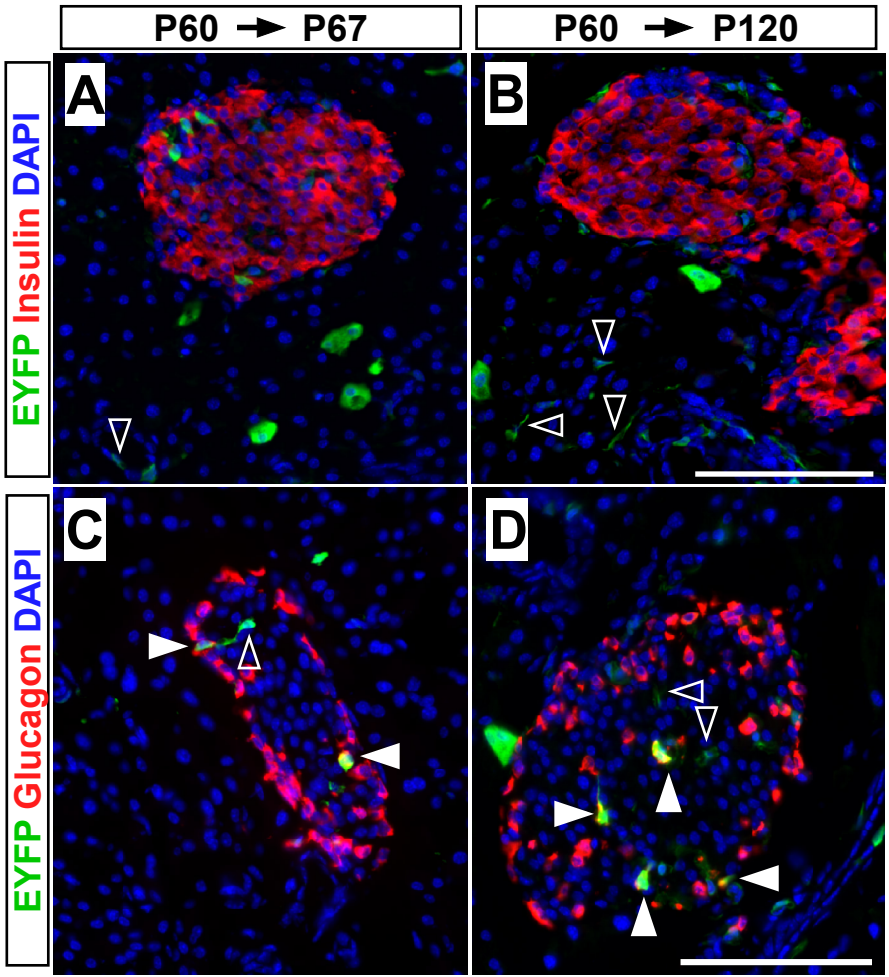
P60 → P67
P60 → P120
A
B
C
D
EYFP Insulin DAPI
EYFP Glucagon DAPI